Available online at www.sciencedirect.com
ScienceDirect
Ore Geology Reviews 31 (2007) 360–383
ORE GEOLOGY REVIEWS
www.elsevier.com/locate/oregeorev

Geological features and origin of the Huize carbonate-hosted Zn–Pb–(Ag) District, Yunnan, South China

Run-Sheng Han [a,b,*], Cong-Qiang Liu [c], Zhi-Long Huang [a], Jin Chen [d], De-Yun Ma [b], Li Lei [b], Geng-Sheng Ma [b]

[a] *Open Laboratory of Ore Deposit Geochemistry, Institute of Geochemistry, Chinese Academy of Sciences, Guiyang 550002, People's Republic of China*
[b] *Kunming University of Science and Technology, Southwest Institute of Geological Survey, Kunming 650093, People's Republic of China*
[c] *Institute of Geochemistry, Chinese Academy of Sciences, Guiyang 550002, People's Republic of China*
[d] *Huize Zn–Pb–(Ag) Mine, Yunnan 654211, People's Republic of China*

Received 3 February 2003; accepted 29 March 2006
Available online 17 July 2006

Abstract

The Huize Zn–Pb–(Ag) district, in the Sichuan–Yunnan–Guizhou Zn–Pb–(Ag) metallogenic region, contains significant high-grade, Zn–Pb–(Ag) deposits. The total metal reserve of Zn and Pb exceeds 5 Mt. The district has the following geological characteristics: (1) high ore grade (Zn + Pb ≥ 25 wt.%); (2) enrichment in Ag and a range of other trace elements (Ge, In, Ga, Cd, and Tl), with galena, sphalerite, and pyrite being the major carriers of Ag, Ge, Cd and Tl; (3) ore distribution controlled by both structural and lithological features; (4) simple and limited wall-rock alteration; (5) mineral zonation within the orebodies; and (6) the presence of evaporite layers in the ore-hosting wall rocks of the Early Carboniferous Baizuo Formation and the underlying basement.

Fluid-inclusion and isotope geochemical data indicate that the ore fluid has homogenisation temperatures of 165–220 °C, and salinities of 6.6–12 wt.% NaCl equiv., and that the ore-forming fluids and metals were predominantly derived from the Kunyang Group basement rocks and the evaporite-bearing rocks of the cover strata. Ores were deposited along favourable, specific ore-controlling structures. The new laboratory and field studies indicate that the Huize Zn–Pb–(Ag) district is not a carbonate-replacement deposit containing massive sulphides, but rather the deposits can be designated as deformed, carbonate-hosted, MVT-type deposits. Detailed study of the deposits has provided new clues to the localisation of concealed orebodies in the Huize Zn–Pb–(Ag) district and of the potential for similar carbonate-hosted sulphide deposits elsewhere in NE Yunnan Province, as well as the Sichuan–Yunnan–Guizhou Zn–Pb–(Ag) metallogenic region.

Keywords: MVT deposit; Carbonate-hosted Zn–Pb–(Ag) sulphide deposit; Huize Zn–Pb–(Ag) district; Yunnan; China

1. Introduction

Deposits of the Huize Zn–Pb–(Ag) district in NE Yunnan Province, P.R. China are typical of many important medium- to large-size, high-grade, Zn–Pb deposits in the Sichuan–Yunnan–Guizhou Zn–Pb–(Ag)

* Corresponding author. Institute of Southwest Geological Survey, Kunming University of Science and Technology, Kunming 650093, People's Republic of China. Tel.: +86 0871 5180377; fax: +86 0871 5111761.
E-mail address: hrs331@sohu.com (R.-S. Han).

0169-1368/$ - see front matter © 2006 Elsevier B.V. All rights reserved.
doi:10.1016/j.oregeorev.2006.03.003

metallogenic province. The region contains about 80 Zn–Pb–(Ag) deposits, including seven large Zn–Pb–(Ag) deposits in NE Yunnan. This metallogenic region has become one of the major producers of Zn–Pb–(Ag) in China (Fig. 1).

The Huize Zn–Pb–(Ag) deposits have played a major role in the development of the non-ferrous industry of China and have been exploited for 50 years from two principal mines (Qilinchang and Kuangshanchang). The district, with its high Zn–Pb–(Ag) grade and presence of

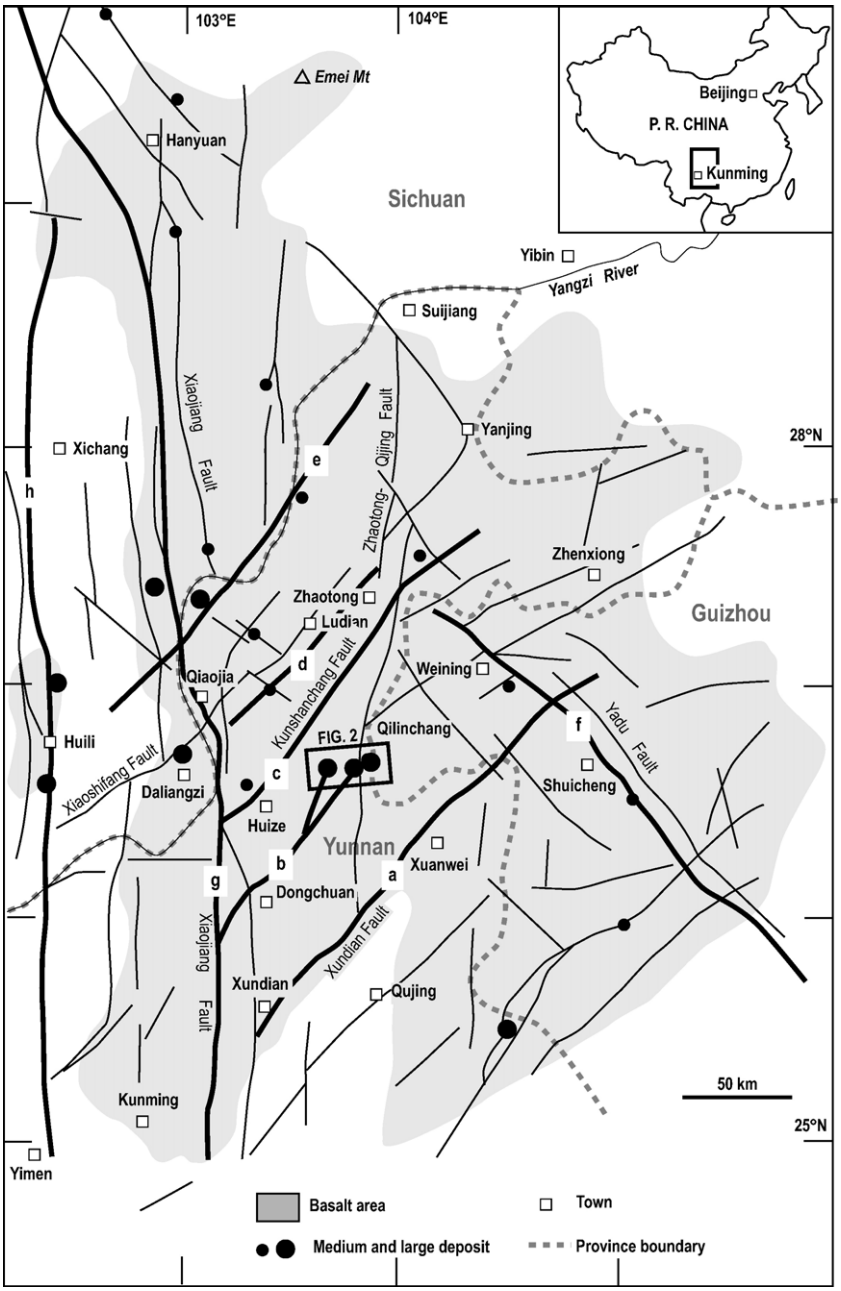

Fig. 1. Tectonic map of the Sichuan–Yunnan–Guizhou Zn–Pb–(Ag) metallogenic zone and the distribution of Zn–Pb–(Ag) deposits. Major NE-trending tectonic zones: (a) the Xundian–Xuanwei fault zone; (b) the Dongchuan–Zhenxiong fault zone; (c) the Huize–Yiliang fault zone; (d) the Ludian–Yanjin fault zone; (e) the Yongshan–Suijiang fault zone. Major NW-trending tectonic zone: (f) the Weining–Shuicheng fault zone. Major NS-trending tectonic zones: (g) the Hanyuan-fault Qiaojia zone; (h) the Xichang–Yimen fault zone.

by-product elements such as Ag, Ge, Cd, Tl and In, has attracted considerable attention from geological researchers. The region has also attracted significant mineral exploration activity. From the 1950s until to the mid-1970s, the Geological Team under the Southwest Non-Ferrous Geological Exploration Bureau carried out geological exploration in the mining district and identified proven Zn and Pb metal reserves (at that time) totalling >1.13 Mt. Between 1984 and 1989, proven Zn and Pb reserves were about 0.2 Mt in the Kuangshanchang area alone (Compiling Committee of the Discovery History of Ore Deposits in China, 1998). In 1993, The No. 6 orebody was discovered at depth in the Qilinchang area, with Zn and Pb metal reserves of 0.78 Mt. During 1997–2001, the concealed No. 8 and 10 orebodies were found in the Qilinchang mining district (including the Dashuijing deposit) using a tectono-geochemical exploration method (Han et al., 1999; Luo, 2000, 2001; Han et al., 2001a,b). Total metal reserves of the Huize Zn–Pb–(Ag) district have been defined at more than 5 Mt, grading ≥25 wt.% (Zn+Pb), ranking the district among the 50 largest Zn–Pb–(Ag) deposits in the world.

Despite the considerable number of studies on the Huize Zn–Pb–(Ag) district over the last decades, there is no consensus about the genesis of the Huize deposits, as well as others in the Yunnan–Sichuan–Guizhou Zn–Pb metallogenic region. In the 1950s, the main genetic hypothesis was a "magmatic–hydrothermal origin." This hypothesis speculated that ore-forming hydrothermal solutions ascended along regional pre-ore faults, and that ore minerals were precipitated at loci favourable to ore deposition. There was, nevertheless, no direct metallogenetic evidence to support this hypothesis. In the 1960s, Xie Jiarong suggested that deposits of this type may be genetically connected with basaltic magmatism and were considered as "post-magmatic hydrothermal deposits". Although Zn–Pb veins in the Fuke basalt at Xuanwei are the only direct evidence in the region linking mineralisation to basaltic magmatism, this hypothesis had a far-reaching influence on later studies. In the 1970–1980s, Liao (1977,1984) supported the hypothesis of a "diverse source" of ore-forming materials and postulated that all Zn–Pb–(Ag) deposits hosted in the Late Sinian (850 to 545 Ma at the base of Cambrian), Late Devonian, Early Carboniferous, and Permian carbonate rocks in NE Yunnan and NW Guizhou Provinces belong to the same genetic type of hydrothermal–sedimentary deposits that were associated with sulphate brines, and further, that these sulphate brines were post-diagenetic. In the 1980s, ore genetic studies were undertaken by Academician Prof. Tu Guangzhi in the Yunnan–Sichuan–Guizhou Zn–Pb–(Ag) metallogenic region. He proposed the theory of "stratabound ore deposits" (Tu, 1984, 1987, 1988), considering that all the Zn–Pb–(Ag) deposits in the region were syngenetic. Tu assigned the genesis of the Huize Zn–Pb–(Ag) district to a "sedimentary-reworking origin."

Other early ore genetic hypotheses for the formation of the Zn–Pb–(Ag) deposits in the Sichuan–Yunnan–Guizhou Zn–Pb–(Ag) metallogenic region include: (1) "hot water sedimentary origin" (Zhang, 1984); (2) "sedimentary-reworking closely associated with micro-facies carbonate rocks" (Zhang, 1989); (3) "Emeishan basalt magmatic hydrothermal mobilisation and enrichment during Indosinian–Yanshanian tectonic localisation" (Shen, 1988); and (4) "rift-related tectonic and rift transformation-reworking" (Zhang and Yuan, 1988). In the 1990s, scholars proposed additional hypotheses such as "sedimentation and post-diagenesis hydrothermal reworking and superimposition" (Chen, 1993b), "sedimentation-reworking" (Zhao, 1995), "sedimentation, reworking, and epigenesis" (Liu, 1996; Liu and Lin, 1999), "deeply-circulating geothermal water filling and epigenetic stratabound" genesis (Shao, 1995), and "convection–circulation metallogenesis and hydrothermal cave" genesis (Zhen, 1997). Zhou (1996) and Zhou et al. (1997, 2001) concluded that the Qilinchang deposit was derived from a MVT-style genetic event, and that the metals were mainly sourced from the Early Sinian igneous suite, although no strong evidence was presented to support this hypothesis. Han et al. (2001c) put forward the "injection and extraction-control" hypothesis and considered that the Huize Zn–Pb–(Ag) district was formed from an ore fluid (probably associated with metamorphic water from the basement rocks) that extracted ore-forming materials from evaporite rocks at depth and concentrated the ores in favourable fault structures.

It is generally accepted that the Huize Zn–Pb–(Ag) deposits have a multi-source origin. The most commonly advocated hypothesis is "sedimentation-reworking," and the main difference among the interpretations presented is that some authors emphasise the contribution of sedimentation processes to metallogenesis and consider that the Palaeozoic strata are the main metal source, whereas others emphasise the contribution of a reworking process and believe that the principal ore-forming metals were derived from a deeper source. In the 1990s, the prevailing hypothesis was "deep superimposition metallogenesis," which suggested a close genetic connection between metallogenesis and basaltic magmatism. The different hypotheses discussed above, although proposed at different times, have mostly focused on regional aspects of Metallogenesis. Few deposit-specific research studies have been carried out on the Huize Zn–Pb–(Ag) district. Although previous hypotheses do not completely explain the genesis of the ore deposits, the numerous ideas put forward allow for a better perspective on the Huize metallogenesis, and have

attracted additional, new research in the area. This paper presents the unique geological features of the Huize Zn–Pb–(Ag) deposits and discusses ore genesis based on new geochemical, isotopic and fluid inclusion data, as well as a compilation of data from previous workers.

2. Geological setting

Geotectonically, the Huize Zn–Pb–(Ag) district is located in the south-central Yunnan–Sichuan–Guizhou Zn–Pb–(Ag) metallogenic region at the southern margin of the Yangtze Craton, and in the southern part of the north-eastern Yunnan Basin on the eastern side of the Xiaojiang deep fault zone (Kang, 1982). Regionally, the district lies at the intersection of NE-, NS- and NW-trending tectonic belts between the Xiaojiang fault zone and the Zhaotong–Qujing concealed fault zone (Fig. 1). The ore district is localised within the Kunshanchang fault zone in the south-western segment of the Dongchuan–Zhenxiong region, which is related to the NS-trending major Xiaojiang and Zhaotong–Qujing faults.

2.1. Stratigraphy

The Huize Zn–Pb–(Ag) district contains the Qilinchang (including Dashuijing) and the large (>1 Mt reserves) Kuangshanchang Zn–Pb–(Ag) deposits, as well as the smaller Yinchangpo Zn–Pb–(Ag) deposit (Fig. 2). These deposits lie above the basement of the Kunyang Group (not exposed) that is composed of low-grade greenschist-facies metamorphic rocks (Han et al., 2000), and overlying Late Sinian and Palaeozoic rocks (Fig. 3). The main stratigraphic sequence in the mine area consists of Middle–Late Devonian, Carboniferous and Permian rocks. The Early Carboniferous Baizuo Formation (C_1b) is the principal ore host sequence (Fig. 4) and is predominantly composed of greyish-white, yellowish-red, and cream-coloured, coarse-crystalline dolomite, compact light-grey limestone, and siliceous dolomitic limestone interbedded with barite.

2.2. Structure

Major faults in the area include the Kuangshanchang, Qilinchang, and Yinchangpo faults, which are spatially related to the Zn–Pb–(Ag) orebodies (Fig. 2) and are all characterised by multiple movements. Five fault orientations are present in the district: NE-, NW-, SN-, NNW-and EW-trending. The mechanical characteristics within the faults and the changes in their attitude suggest that they have undergone five episodes of tectonic movement (Han et al., 2001d). The orientation and sequence of evolution and development of tectonism from Jinningian

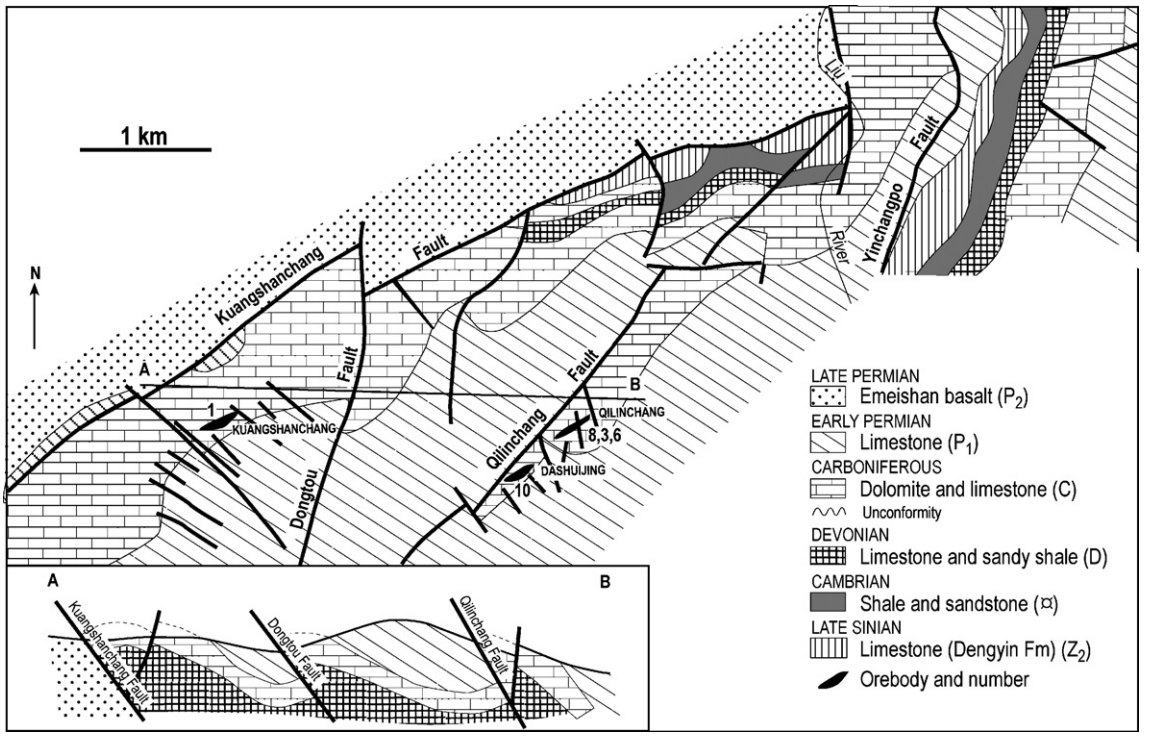

Fig. 2. Generalised map and cross-section through the Huize Zn–Pb–(Ag) district (modified after data up to 1998 from the Huize Zn–Pb–Ag Mine).

Era	System	Formation	Thick-ness (m)	Lithological character
Upper Palaeozoic	Permian	Basalt (P_2)	600-800	Greyish-green, compact-massive, amygdaloidal basalts, the middle and upper parts are purple altered basalts with leaf-like native Cu between them, in pseudo-conformable contact with the underlying strata.
		Qixia-Maokou (P_1q+m)	450-600	Dark light grey limestone, dolomitic limestone intercalated with dolomite, dolomitic materials unevenly distributed.
		Liangshan (P_1l)	20-60	Upper: greyish black carbonaceous shale/fine sandstone, intercalated with coal. Lower: yellowish white sandstone intercalated with yellowish brown argillaceous shale.
	Carbon-iferous	Maping (C_3m)	27-85	Upper: pisolitic limestone and limestone. Middle: Intercalations of purplish red and yellowish green shale. Lower: Purple, greyish purple brecciated limestone, the breccia cemented by purple, yellowish green argillaceous materials.
		Weining (C_2w)	10-20	Light grey limestone intercalated with oolitic limestone.
		Baizuo (C_1b)	50-80	Middle-Upper: white-white, cream-yellow coarse crystalline dolomite intercalated with light grey dolomitic limestone (the main ore-host bed).
		Datang (C_1d)	5-25	Grey limestone, and oolitic limestone, 0-5 m thick, greyish brown siltstone and purple mudstone at the bottom.
Lower Palaeozoic	Devonian	Zaige (D_3zg)	200-310	Upper: Grey limestone, yellowish white and yellowish red medium-coarse crystalline dolomite (subordinate ore-bearing bed). Pb-Zn orebodies hosted in light coloured coarse crystalline dolomite near Xiaoheiqing. Middle: light grey, medium to thick layered, siliceous dolomite intercalated with greyish yellow, thin layered calcareous shales, light yellow, light yellowish red, fine crystalline dolomite observed locally at the top. Lower: Light grey, medium to thick layered, fine-medium coarse crystalline dolomite intercalated with light grey argillaceous dolomite.
		Haikou (D_2h)	0-11	Light grey, light yellow sandy siltstone/green, greyish black argillaceous shale alterations; in pseudo-conformable contact with the underlying strata.
	Cambrian	Qiongzhushi ($€_1q$)	0-70	Black argillaceous shale intercalated with yellow sandy mudstone and gypsum salt beds, in pseudo-conformable contact with the underlying strata.
Proterozoic	Sinian	Dengying (Z_2dn)	>70	Light grey, greyish white siliceous dolomite, in pseudo-conformable contact with the underlying strata.

Fig. 3. The stratigraphic column of the Huize Zn–Pb–(Ag) district, Yunnan Province, China.

(Neoproterozoic) to Himalayan (Tertiary) time is: (1) NS-trending; (2) NW-trending; (3) NE-trending; (4) NS-trending; and (5) EW-trending. Tectonic zones are characterised by large-scale overthrust structures, folds, and compressional-shear faults. During the different tectonic episodes, the main compressive stress (σ_1) varied from 90° → 45°, to 55° → 300°, to 310° → ~90°→ ~180°.

2.3. Magmatic activity

Magmatic activity in the district is marked by the Late Permian Emeishan basalt (K–Ar ages: 218.6–253.3 Ma) (Figs. 1 and 3) that outcrops on both sides of the Xiaojiang fault zone (Liu, 1996), with 52 main occurrences of intermediate to felsic and mafic to ultramafic rocks in the western part of the district, along the Xiaojiang fault, and 11 main occurrences of mafic rocks in the eastern part of the district, also along the fault (Liu and Lin, 1999). Only one location contains Pb and Zn mineralisation associated with pyritization of the ultramafic rocks. Numerous diabase, gabbro–diabase sills, and dikes (K–Ar ages: 246–283 Ma) lie east of the Xiaojiang fault (Liu and Lin, 1999). The contact zones of some diabase bodies contain intense hydrothermal alteration (i.e., silicification and epidotisation) and Pb, Zn and Cu mineralisation. Spatial distribution of the basalt generally coincides with the distribution of the Zn–Pb–(Ag) deposits and associated mineral occurrences (Fig. 1A).

3. The orebodies

Geological features of the major Zn–Pb–(Ag) orebodies of the Qilinchang (including the Dashuijing),

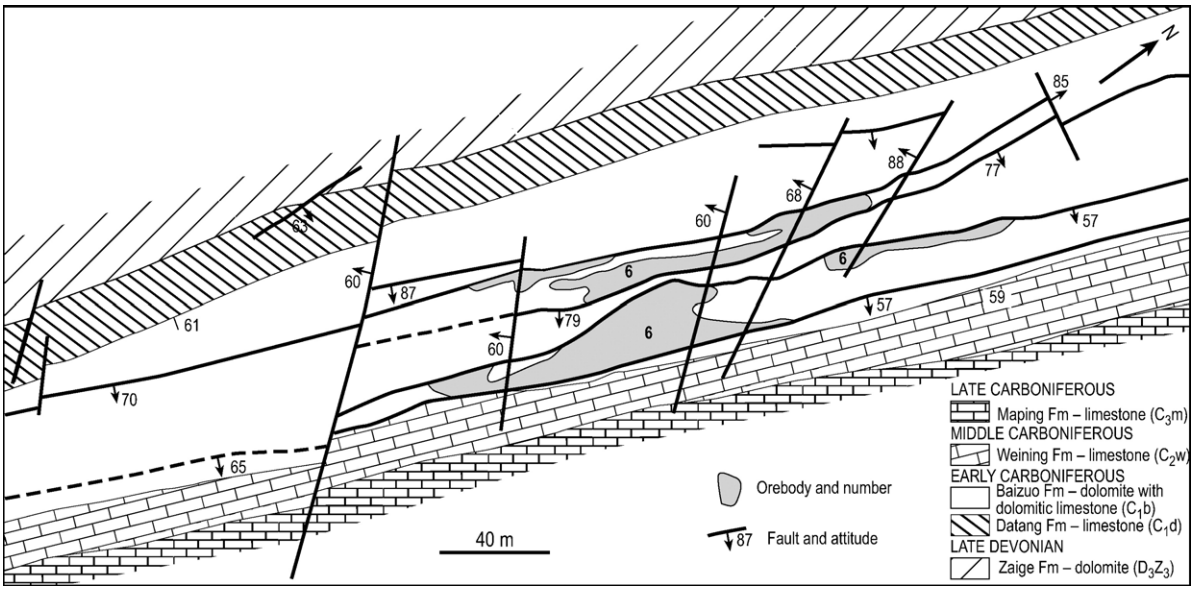

Fig. 4. Plan map of No. 6 orebody at the 1631 level in the Qilinchang Zn–Pb–(Ag) deposit.

Kuangshanchang, and Yinchangpo Ag–Zn–Pb–(Ag) deposits are summarized in Table 1. Fifty orebodies of various sizes are present within the 20 km^2 area that is the Huize Zn–Pb–(Ag) district. This total includes the 42 orebodies that make up the Kuangshanchang deposit, and the 8 orebodies constituting the Qilinchang deposit. Among these, the Nos. 10, 8 and 6 orebodies in the Qilinchang deposit and the No. 1 orebody in the Kuangshanchang deposit are the largest and most important (Table 1, Fig. 2). The large Qilinchang deposit is more than 800 m along strike, 720 m in oblique length, and more than 1200 m along dip, with a thickness varying from 0.7 to 40 m. The orebodies are distributed within an interstratified fault zone between the middle and upper horizons of the Baizuo Formation (Fig. 4). They are stratabound and lenticular in shape and locally

Table 1
Geological features of major orebodies of the Huize Zn–Pb–(Ag) district, Yunnan, China

Major deposit	Metal reserves	Major mineral	Subordinate mineral	Major element	Minor element	Trace element	Major orebody	Average grade of Zn+Pb (%)	Average grade of Ag (ppm)
Qilinchang (including the Dashuijing)	ca. 2 Mt large	Sphalerite, galena, pyrite, calcite, dolomite	Marmatite, barite, gypsum, matildite, boulangerite	Zn, Pb, S, Fe	Cd, As	Ag, Ge, Tl, Mo, Sb, In, Ga	3 6 8	36.5 34.6 25.8	163 111 61
	ca. 1 Mt large	Sphalerite, galena, pyrite, calcite, dolomite	Marmatite barite, quartz, matildite	Zn, Pb, Fe, S	Cd, As	Ag, Ge, Tl, Mo, Sb, In, Ga	10	33.5	71.0
Kuangshanchang	ca. 1.8 Mt large	Sphalerite, galena, pyrite, calcite, dolomite	Marmatite barite, gypsum, matildite, quartz	Zn, Pb, Fe, S	Cd, As	Ag, Ge, Tl, Mo, Sb, Ga, In	1	30.6	89.5
Yinchangpo	<0.3 Mt small	Galena, sphalerite, pyrite, calcite, dolomite, chalcopyrite	Tetrahedrite, native silver, freibergite, chlorargyrite, quartz	Pb, Zn, S, Fe, Cu	Ag, As, Cd	Ge, Tl, Sb, Mo, Ga, In	1 2 3 4	9.1 7.5 12 8.3	310 255 273 235

The distinction between major elements and minor elements or major minerals and subordinate minerals is subjective; typically the minor compositions are less than 1% but more than 0.1%.

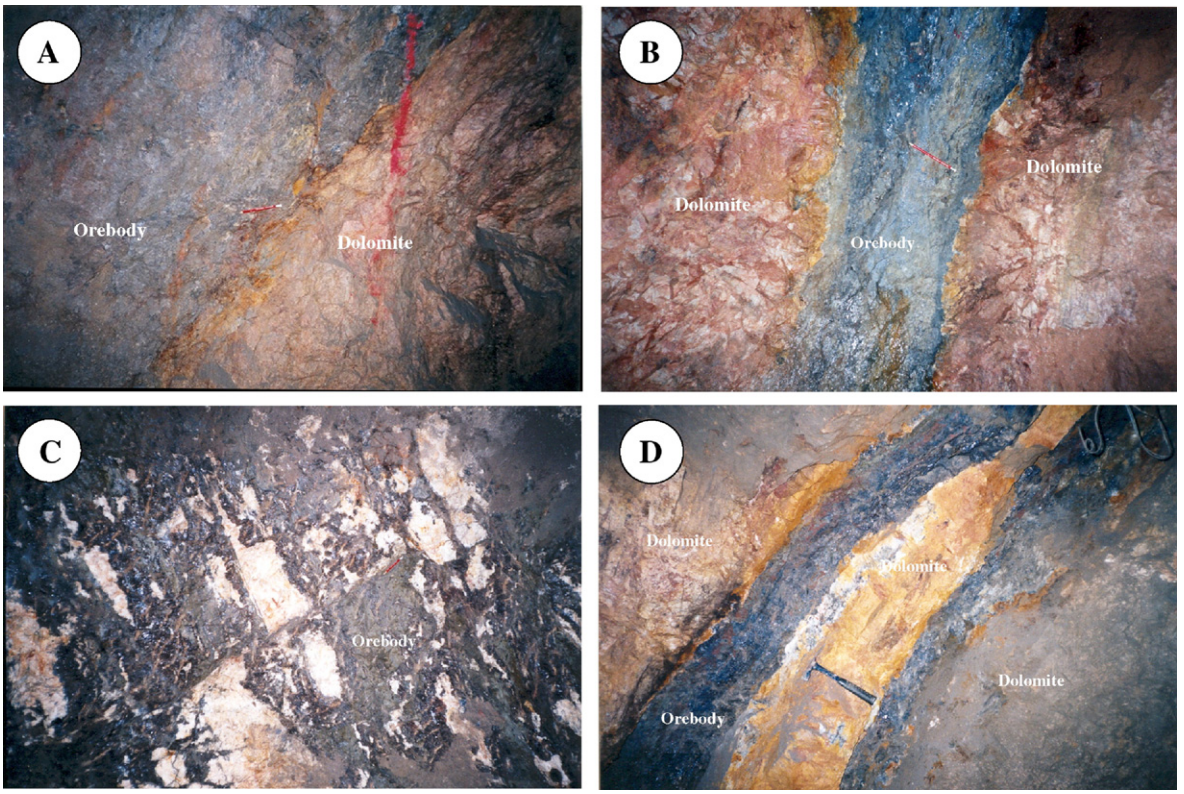

Fig. 5. Field photographs from underground workings of the Huize Zn–Pb–(Ag) deposit, Yunnan, China. (A) Distinctive boundaries between the orebody (grey-black, upside) and the coarse crystalline dolomite wall rock (C_1b, light coloured, underside) in the Qilinchang deposit. (B) Distribution of the Ag–Zn–Pb–(Ag) ore (black) and gangue mineral (calcite, white) at the No. 6 orebody in the Qilinchang deposit. (C) Distribution of the Zn–Pb–(Ag) orebody (black) in the NE interstratified compressional-shear fault zone, and the distinctive boundaries between the orebody and coarse-crystalline dolomite (C_1b, gray-light coloured). (D) Distribution of the Zn–Pb–(Ag) orebody (black, central section) in the NE interstratified compressional-shear fault zone in the coarse-crystalline dolomite (C_1b, grey-light coloured).

pinch and swell. Attitudes are approximately parallel to bedding in the host rocks, striking 20–30°NE and dipping SE at 50–70°. The orebodies have sharp contacts with the wall rocks (Fig. 5A, C and D).

3.1. Ore types and textures

The main ore types are oxide ores in the upper parts, mixed ores containing both oxides and sulphides in middle levels, and sulphide ores in the deeper parts. The ores are divided into two major types: massive ores (including sphalerite ore, sphalerite–galena ore and galena–pyrite ore) and disseminated ores (including sphalerite ore, sphalerite–galena ore and galena–pyrite ore); massive ores are the dominant type.

The principal ore textures are subhedral–euhedral granular, metasomatic-resorption, and fracture-infill textures, as well as graphic, skeletal, and exsolution textures (Fig. 6). Euhedral–subhedral–anhedral granular textures and microcrystalline to coarse-crystalline granular textures are the most common. Ore structures are dominated by massive accumulations of sulphide minerals, but may be veined, disseminated, and brecciated.

3.2. Ore mineralogy

Detailed field and microscopic examinations indicate that the dominant ore minerals in the Huize deposits are galena, sphalerite, and pyrite, with minor chalcopyrite and hopeite, as well as matildite, acanthite, freibergite, and chlorargyrite. Gangue minerals mainly are calcite and dolomite, with minor barite, gypsum, quartz, and clay minerals (Table 1).

Sphalerite is fine to macrocrystalline, anhedral to euhedral, and granular in form (0.05–20 mm). There are three main phases of sphalerite: early sphalerite is dark grey-brown to dark brown, the second generation is light brown, and the late-phase sphalerite is light yellow.

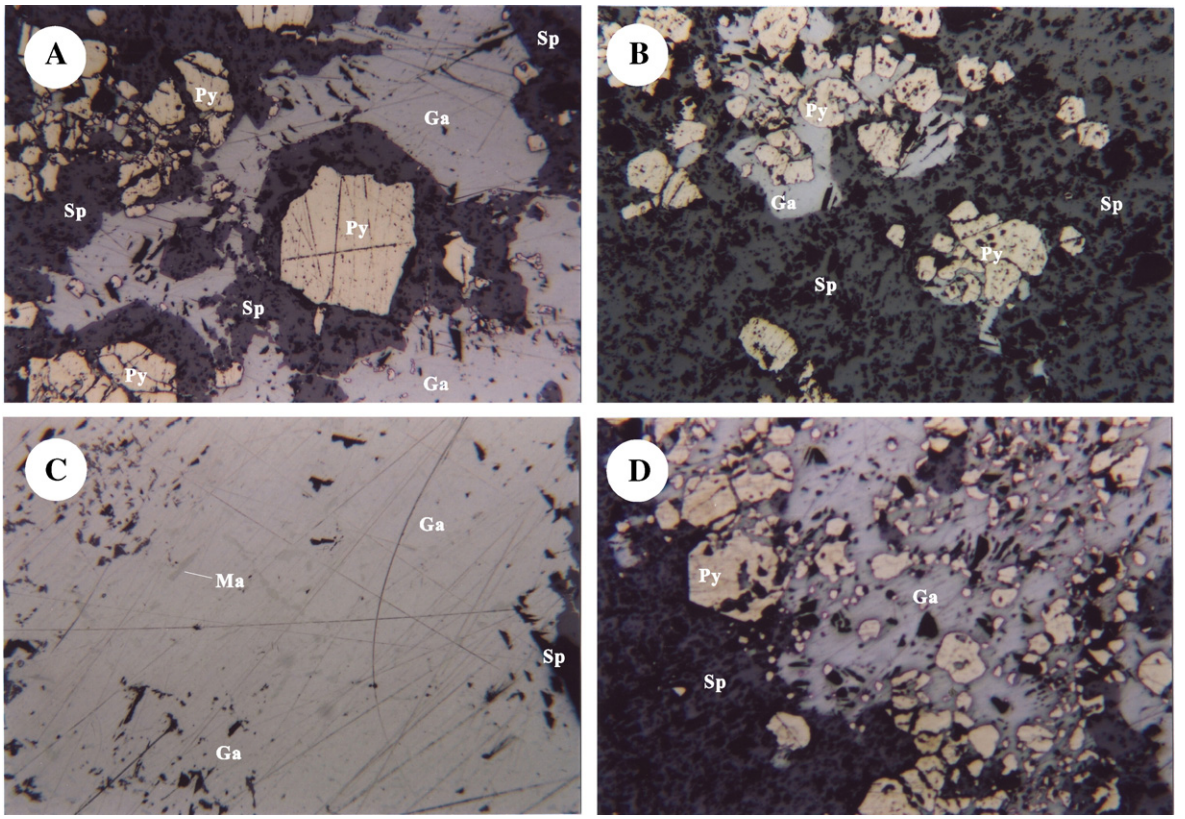

Fig. 6. Photographs of textures and structures of the Huize Zn–Pb–(Ag) ores, Yunnan, China. (A) Massive sphalerite (Sp) (grey) embracing subhedral crystalline pyrite (Py) (light coloured) (0.025–0.25 mm) and galena (Ga) (white) replacing sphalerite. Location: QL-6-1 of the No. 10 orebody in the Qilinchang deposit. Horizontal view: 1.3 mm. (B) Galena (Ga) replacing subhedral–euhedral (0.03 to 0.15 mm) pyrite (Py), exhibiting estuary texture and metasomatic-resorption texture. Both the minerals are distributed in sphalerite (Sp) (grayish green). Location: QL-53 of the No.10 orebody in the Qilinchang deposit. Horizontal view: 1.3 mm. (C) Matildite (Ma) (light grey) (4×25 μm) and galena (Ga) exhibiting solid solution texture in galena (white), galena aggregate replacing sphalerite (Sp) (grey). Location: QL-97-01 of the No. 10 orebody in the Qilinchang deposit. Horizontal view: 0.6 mm. (D) Subhedral–euhedral pyrite (Py) (light yellow) pentagonal dodecahedron (0.025–0.25 mm) replaced by galena (Ga) (white), exhibiting metasomatic-resorption texture; sphalerite (Sp) (grey) distributed in the periphery. Location: QL-111 of the No. 10 orebody in the Qilinchang deposit. Horizontal view: 2.5 mm.

Sphalerite forms as massive, banded, and disseminated aggregates coexisting with galena, pyrite, and calcite. The mineral is sometimes present within skeletal crystals of pyrite, which exhibit 'estuary', relic, and containment textures (Fig. 6A, B, and D). An exsolution texture of matildite and galena replacing sphalerite is also observed (Fig. 6C). Large, coarse-grained (0.25–5 mm) sphalerite crystals are common within corrosion cavities. In addition, zoned growth textures are also present.

Galena is present as fine- to coarse-grained, anhedral granular aggregates, 0.2–20 mm in size. Stress deformation is obvious, and exsolution textures are common (Fig. 6C). Galena generally coexists with sphalerite, pyrite, and calcite.

Pyrite occurs in four main textural types. Anhedral to subhedral, granular and sometimes colloform pyrite formed early during sedimentation. Second-stage pyrite is coarse-grained, euhedral and granular, 2–5 mm in size, with crystals dominated by combinations of pentagonal–dodecahedra and pentagonal–dodecahedron–cubic forms. Second-stage pyrite is present as massive, disseminated, and banded aggregates and is distributed mainly within the country rocks adjacent to the orebodies. Third-stage pyrite is medium- to coarse-grained and dominated by grains with pentagonal dodecahedra shape. Late-stage pyrite is present as fine-grained cubes, 0.01–0.5 mm in size, and local pentagonal–dodecahedra, mostly present within dolomite in the hanging wall of the orebodies or in fault zones near the orebodies. Pyrite is sometimes present in microveinlets and networks along fissures in galena and sphalerite. Away from the orebodies, pyrite becomes more abundant.

Dolomite is present as coarse-grained crystals, 0.l–1 mm in grain size, exhibits euhedral–subhedral granular textures, and shows distinctive signs of carbonate recrystallisation. It locally replaces pyrite, giving the pyrite a skeletal texture. Calcite is mainly present as massive, banded, vein and disseminated forms within the orebodies and in the mineralised dolomite of the Baizuo Formation, as well as in the NW-striking fault zone.

4. Metallogenic periods and stages

Processes affecting the Huize Zn–Pb–(Ag) district have been divided into: (1) a sedimentary diagenetic stage, (2) a hydrothermal ore-forming stage, and (3) a stage of epigenesis (Fig. 7). The economic deposits were formed during the hydrothermal ore-forming stage.

4.1. Tectonic evolution

The region of NE Yunnan has a protracted geological and tectonic history, which is described as development during a "two-layer" evolution, in which the two layers are composed of the lower basement (Proterozoic) and the overlying Palaeozoic cover rocks; the tectonic evolution of the two differing from one another. The regionally exposed basement rocks are composed of the Proterozoic Kunyang Group consisting of sandy slate, phyllite and carbonate rocks, the Early Proterozoic Kangding Group containing amphibolite gneiss, migmatite and felsic gneiss, and the Archaean–Early Proterozoic Danghongshan Group of greenschist–facies clastic rocks and spilite–keratophyre series. The Early Proterozoic rocks show intense tectonic deformation textures. The underlying Archaean rocks contain fabrics that suggest three distinct phases of deformation. The tectonic orientation of the first deformation phase is mainly NS-trending and is often overprinted by the second phase. The second deformation phase was a penetrative, intense deformation of the basement, with an EW-trending tectonic orientation. The third deformation phase was not extensive, and is marked by conjugate shear zones and folds with fold axes that are randomly oriented, but partly NS-trending. The Kunyang Group strata, exposed between the Yuanmu–Luzhijiang and the Xiaojiang fault zones, are a suite of slightly metamorphosed clastic rocks and carbonates, which strike N–S. The volcanic rocks, intercalated between the two fault zones, are enriched in alkalis and are characterised by a

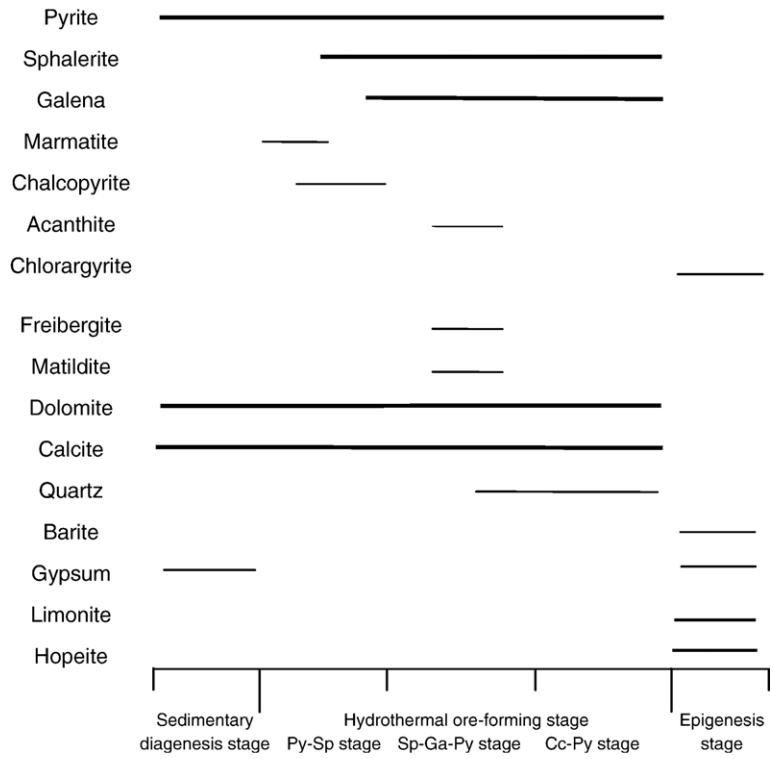

Fig. 7. Metallogenic stages and mineral-forming sequence of the Zn–Pb–(Ag) deposits in the Huize Zn–Pb–(Ag) district, Yunnan, China. Py–pyrite; Sp–sphalerite; Ga–galena; Mar–'marmatite'; Cc–calcite.

bimodal-type suite that was affected by tensional stresses. It contains Pb- and Zn-rich layers widely distributed across the region (Liu and Lin, 1999). The Jinningian movement resulted in the formation of NS- and NE-trending fold and fault zones, marking the end of basement deformation.

Tectonic evolution of the cover rocks occurred after the Jinningian movement, as this region entered a period of platform sedimentation. Because the region lies within the transitional zone between the Kangdian Axis and East Yunnan sag zone within the Yangtze block, tectonic movement prior to the Himalayan Orogeny was generally characterised by tensional and vertical ascending and descending movements. Syntectonic sedimentation caused the stratigraphic sequences to be highly variable both in thickness and in sedimentary facies type. From the Sinian to Early Cambrian, a thick clastic and carbonate wedge formed, which was intercalated with finely layered evaporitic rocks (Liu and Lin, 1999). From the Middle Cambrian to Early Permian, tectonism was multi-episodic with vertical movements. This caused a number of changes in sedimentation thickness and in sedimentary facies, and produced a number of stratigraphic discontinuities within the sequence.

During the Carboniferous, the Huize Zn–Pb–(Ag) district was located in an area of extensive marine sedimentation, resulting in deposition of the Baizuo Formation in a restricted basin in the Kunyang–Zhaotong area (Chen, 1993a), adjacent to the Upper Yangtze Craton, and located in the NW part of the Huize Zn–Pb–(Ag) district. The district was therefore within a lagoonal subfacies, positioned between tidal flat subfacies and the interbeach subfacies. Sedimentation resulted in a suite of carbonate-bearing formations in the basin that characterise the host rocks of the Zn–Pb–(Ag) deposits (Chen, 1993a). During the Late Permian, the region was subjected to extensional tectonism, a period that also featured extensive thick basalt flows. Since the Late Permian, crustal movement changed from tensional, dominated by vertical movement, to a close-to-horizontal compressional domain. Consequently, a number of NS-, NE- and NW-trending tectonic zones were formed and were accompanied by magmatism. This was the principal period of Zn–Pb–(Ag) ore formation in this region. During the Tertiary Himalayan Orogeny and uplift of the Yunnan–Guizhou Plateau, this region again underwent E–W extension, resulting in a series of N–S-trending fault-bounded basins and tensional fault systems. These fault systems have led to the offset of many of the Zn–Pb–(Ag) orebodies. The development and configuration of the structures in the cover rocks in NE Yunnan was also controlled by structures in the basement.

5. Metallogenic and geochemical characteristics

Detailed studies of the structural and geochemical controls of the origin of the Huize deposits by Han et al. (2001c,d) indicate that the district possesses unique metallogenic characteristics that allowed development of the rich Zn–Pb–(Ag) deposits. The district is characterised by a particularly high ore grade (Tables 1 and 2), thick orebodies (up to 30 m or more), and by a simple ore mineral assemblage (sphalerite, galena, pyrite and calcite as the major gangue mineral; Fig. 5B). The No. 10 orebody is particularly massive. The thickness and tonnage of the orebodies tend to progressively increase with depth.

Table 2
Contents (wt.%) of major elements in the ores from the Huize Zn–Pb–(Ag) district, Yunnan, China

Sample number	Ore type	SiO_2	TiO_2	Al_2O_3	TFe	MnO	MgO	CaO	Na_2O	K_2O	P_2O_5	CO_2	IT	Zn	Pb	S	Σ
HQ-93	Zn–Pb ore	1.10	0.03	0.09	27.20	0.04	0.50	1.10	0.04	0.04	0.002		0.70	30.09	10.92	27.61	99.46
HQ-94	Zn–Pb ore	1.05	0.35	0.47	38.00	0.06	0.60	1.90	0.04	0.03	0.001		0.80	14.32	7.75	34.28	99.65
HQ-84	Zn–Pb ore	1.36	0.22	0.23	29.70	0.14	0.40	2.20	0.03	0.01	0.001		0.75	23.25	11.28	30.30	99.87
HQ-95	Zn–Pb ore	2.35	0.37	0.14	17.40	0.05	0.50	2.60	0.03	0.09	0.001		0.60	34.35	11.75	29.25	99.48
HQ-99	Zn–Pb ore	3.68	0.45	0.94	24.10	0.15	0.80	8.30	0.03	0.2	0.003	0.80	1.70	20.71	10.58	27.25	99.69
HQ-108	Zn–Pb ore with dolomite	1.82	0.10	0.47	16.60	0.08	6.00	10.20	0.04	0.03	0.003	3.90	7.97	18.55	9.64	23.88	99.28
HQ-109	Zn–Pb ore with dolomite	2.18	0.42	0.94	14.50	0.12	1.40	12.10	0.05	0.18	0.001	7.95	4.95	19.15	8.70	26.60	99.24

Analytical unit: Open Laboratory of Ore Deposit Geochemistry, Institute of Geochemistry, Chinese Academy of Sciences, P.R. China.
The contents of major chemical composition and those of Pb, Zn and S in the ores were analyzed by wet chemistry. TFe = Fe_2O_3 + FeO.
All samples were ground as fine as −200 meshes under a contamination-free environment and were prepared as super-pure samples by the Laboratory of Research Department of Geological Fluids, Institute of Geochemistry, Chinese Academy of Sciences, P.R. China.

5.1. Enrichment in Ag and other accessory elements

In addition to Pb, Zn, Fe and S, the ores also contain a range of minor trace elements including Ag, Ge, Cd, In, Ga, and Tl. Among these Ag, Ge, Cd, Tl and In are of economic importance, making the Huize Zn–Pb–(Ag) district not only a Zn–Pb–(Ag) district, but, in restricted parts, also a significant producer of Ag and Ge. Concentrations of these by-products are as follows: up to 200 ppm Ag, up to 81.34 ppm Ge, up to 488.0 ppm Cd, up to 2.55 ppm In, up to 1.93 ppm Ga and up to 11.85 ppm Tl (Table 3). Titley (1993, 1996) suggests that, in MVT-type deposits, the Ag content increases with formation temperature; this may also apply to the Huize Zn–Pb–(Ag) district.

Silver and other trace elements are unevenly distributed among the major ore minerals (Table 4). Silver contents are the highest (76–144 ppm) in galena and are associated with Tl and Cd, as well as minor Ge. Sphalerite concentrates Cd, Ge, and Ag and trace amounts of In, Ga, and Tl. The different varieties of sphalerite contain varying concentrations of Ge and Ag. Early sphalerite has the highest Ge and Cd concentrations (Ge: 115–178 ppm; Cd: 770–1048 ppm) and also higher concentrations of Ag (18–67 ppm). Concentrations of Ge and Ag in late sphalerite range from 1 to 88 ppm and 6–35 ppm, respectively. Pyrite contains Tl and Ag. Early-stage pyrite contains low concentrations of Tl and Ag (Tl: <1.61 ppm; Ag: <6.4 ppm); the second- and third-stage pyrites contain higher concentrations of Tl and Ag (up to 3234 ppm Tl and 17.14 ppm Ag). In summary, galena is the major carrier of Ag and an important carrier of Tl and Cd; sphalerite is the major carrier of Ge and Cd and a important carrier of Ag, In, and Ge. The second- and third-stage pyrites are the major carriers of Tl and an important carrier of Ag.

5.2. Wall-rock alteration and metal zonation

Styles of wall rock alteration in the Huize Zn–Pb–(Ag) deposits are relatively simple. Except for intensive dolomitisation, which is widespread in the middle–upper parts of the Baizuo Formation, hydrothermal alteration is expressed by the presence of sparse silica, pyrite, and clay minerals in the orebodies and the country rocks close to ore. MgO, TiO_2, Fe_{tot}, K_2O, SiO_2 and Al_2O_3 are all enriched in altered wall rock (Table 5). Dolomite occurs in coarse-crystalline, granular, massive, and irregular forms and is distributed in the mineralised and altered zones and orebodies. Altered dolomite is white, greyish-white, cream-yellow and yellowish-pink in colour. Dolomite dissolution cavities are widely developed and display a gradual relationship from distinct relics within limestone to dolomitic limestone. Networks of dolomite veinlets are commonly distributed within these relics. The intensity of dolomitisation increases with increased depth, size, ore grade, and thickness of orebodies. Silicification is relatively weak and is present only in the immediate footwall and the hanging wall of the orebodies.

Mineral assemblages in the main orebodies are zoned from foot- to hanging wall as follows: coarse-crystalline pyrite and 'marmatite' → sphalerite, galena and pyrite → finely crystalline pyrite and carbonate minerals. The finely

Table 3
Contents (ppm) of trace elements in the ores from the Huize Zn–Pb–(Ag) district, Yunnan, China

Sample number	Ore type	Cu	Ga	Ge	As	Mo	Ag	Cd	In	Sb	Au	Tl
(NBS-1633a)[a]	(Standard sample)	111.1	53.34	32.90	139.5	26.74	0.619	0.836	9.531	6.518	0.050	5.653
(NBS-1633a)[b]	(Standard sample)	118	58	33.9	145	29	0.076	1	0.16	6.8	0.052	5.7
HQC-84	Zn–Pb ore	171.2	2.563	46.44	1714.0	2.723	78.05	354.3	0.682	227.5	0.007	4.176
HQC-93	Zn–Pb ore	124.2	1.720	57.33	1087.0	4.429	74.17	380. 9	0.331	115.5	nd	4.180
HQC-94	Zn–Pb ore	116.3	4.342	6.380	1689.0	0.460	45.94	233.0	0.676	67.12	0.026	3.409
HQC-95	Zn–Pb ore	401.4	1.633	81.34	454.3	3.792	100.6	488.0	0.915	207.8	0.010	6.223
HQC-99	Zn–Pb ore	140.8	2.322	30.32	730.8	0.402	81.51	298.9	0.847	122.9	0.011	6.193
HQC-108	Zn–Pb ore with dolomite	154.0	1.922	42.84	467.0	2.222	81.07	261.9	0.864	210.1	0.018	4.388
HQC-109	Zn–Pb ore with dolomite	156.9	2.967	54.05	473.7	0.921	78.47	369.4	1.006	153.9	nd	3.476
QLC-128	Zn–Pb ore	40.40	0.846	9.740	357.2	0.583	54.19	354.9	0.086	112.2	nd	11.03
QLC-129-1	Zn–Pb ore	73.70	4.830	20.33	239.6	1.996	34.45	5198	0.050	35.17	nd	7.079

Analytical unit: Open Laboratory of Ore Deposit Geochemistry, Institute of Geochemistry, Chinese Academy of Sciences, P.R. China.
The contents of trace elements (ppm) analysed by ICP-MS techniques and method after Qi et al. (2000).
Detection limits of elements (ppm): Cu: 0.37; Ga: 0.026; Ge: 0.1; As: 1; Mo: 0.061; Ag: 0.05; Cd: 0.005; In: 0.001; Sb: 0.05; Au: 0.001; Tl: 0.02
nd, not detected.
All samples were ground as fine as −200 meshes under a contamination-free environment and were prepared as super-pure samples by Laboratory of Research Department of Geological Fluids, Institute of Geochemistry, Chinese Academy of Sciences, P.R. China.
[a] Standard sample from China.
[b] Standard sample from Korotev (1996).

Table 4
Contents of trace elements (ppm) of ore minerals in the Huize district, Yunnan, China

Sample number mineral	HQ-498 Py (3)	HQ-493C Py (3)	HQ-491 Py (3)	HQ-503C Py (2)	HQ-487 Py (3)	Q-480 Py (2)	HQ-473X Py (1)	HQ-488 Py (3)	HQ-493X Py (3)	HQ-495 Py (3)	HQ-485 Py (2)	HQ-483 Py (2)	HQ-490 Py (3)
Ga	0.037	0.102	0.002	nd	nd	0.177	0.3	0.033	nd	0.001	0.083	0.192	0.023
Ge	0.585	0.37	0.494	0.288	0.356	0.291	0.379	0.487	0.694	0.471	0.26	0.534	0.504
Ag	3.274	3.203	8.224	3.986	5.596	1.892	1.256	4.585	8.297	2.68	3.742	6.4	10.70
Cd	0.617	1.769	4.171	0.553	2.262	0.896	0.774	0.98	1.79	2.429	0.764	1.453	1.368
In	0.011	0.008	0.008	0.018	0.021	0.017	0.082	0.011	0.007	0.015	0.025	0.098	0.024
Tl	304.5	383.3	3234	1481	1975	0.503	0.769	1202	2680	539.0	316.5	0.841	3256
Location	No. 10 orebody of the Qilinchang deposit												
Sample number mineral	HQ-491 Sp (2)	HQ-490 Sp (2)	HQ-493 Sp (1)	HQ-488 Sp (2)	HQ-495 Sp (1)	HQ-498 Sp (1)	HQ-487 Sp (2)	C2W-1 Py (2)	1571-1 Py (3)	1571-9-9 Py (3)	1571-9-1 Py (3)	HQ-84 Ga	28-2 Sp (2)
Ga	3.441	7.92	2.078	5.568	2.806	13.218	1.701	0.427	0.525	0.29	0.363	nd	1.67
Ge	87.59	60.26	141.26	53.25	115.14	105.35	58.93	0.24	0.478	0.87	0.959	0.042	7.616
Ag	34.89	23.76	40.68	29.40	67.06	41.13	22.35	2.277	14.05	17.14	26.56	75.841	10.94
Cd	833.5	701.6	769.9	766.2	804.8	991.4	752.4	0.186	0.853	4.023	11.33	3.919	794.0
In	0.186	0.35	0.341	0.2	0.383	0.561	0.126	0.006	0.042	0.023	0.029	0.01	1.634
Tl	1.941	1.048	4.605	1.63	9.192	2.356	1.028	0.031	1.499	3.614	11241	2.867	1.159
Location	No. 10 orebody of the Qilinchang deposit							No. 6 orebody of the Qilinchang deposit					
28-3 Sp (1)	28-1 Sp (3)	MQ-1053 Py (1)	MQ-908 Py (1)	MQ-910 Py (3)	MQ-911 Py (3)	MQ-912 Py (2)	MQ-915 Py (2)	MQ-918 Py (2)	MQ-919 Py (3)	MQ-909 Ga	MQ-910 Ga	MQ-911 Ga	MQ-916 Ga
0.412	0.474	1.109	0.204	0.23	0.226	0.19	0.273	0.129	0.29	nd	nd	nd	nd
177.8	1.187	0.471	0.737	4.026	0.531	0.249	0.731	0.316	2.294	5.439	2.126	1.173	1.316
18.26	6.027	1.1	2.073	35.80	10.79	1.703	7.136	7.625	23.07	103.15	144.5	104.4	134.41
1048	787.2	0.871	2.364	15.06	2.367	0.086	3.123	5.411	11.20	37.04	24.43	8.12	10.34
0.096	0.203	0.154	0.013	0.054	0.04	0.014	0.01	0.018	0.034	0.003	0.018	0.013	0.004
1.47	1.131	1.614	0.281	6.202	2759	266.7	1.967	4.592	3.76	29.55	27.62	26.64	27.8

Analytical unit: Open Laboratory of Ore Deposit Geochemistry, Institute of Geochemistry, Chinese Academy of Sciences, P.R. China.
The contents of trace elements (ppm) by ICP-MS techniques and method after Qi et al. (2000).
Method of sample processing, detection limits of elements (ppm) and standard samples are same as Table 3.
Py–pyrite; Sp–sphalerite; Ga–galena; the numbers in the parentheses are the mineral stages.

crystalline pyrite is enriched along the contact between the wall rock and the orebody. This zonation is compatible with primary gravity settling and separation during ore formation, such that heavier minerals ('marmatite', sphalerite, galena, etc.) are typically centralised along the bottom and the central parts of the orebody, whereas lighter minerals (calcite, etc.) are concentrated near the upper parts of the orebody.

6. Structural and lithological control

6.1. Structural control

The Xiaojiang and the Qujing–Zhaotong fault zones are the regional-scale ore-controlling structures in the Sichuan–Yunnan–Guizhou Zn–Pb–(Ag) metallogenic zone. The Xiaojiang fault zone is a supercrustal fault zone that resulted from a prolonged evolution of movement. The fault zone constitutes the eastern boundary of the NS-trending overthrust faults of the Proterozoic Kunyang rift. Intense limonitization and the structural features also suggest multiple episodes of tectonic activity. On the western side of the fault zone, recent discoveries of Zn, Cu, and Pb have been reported (Table 6); Pb grades may locally exceed 15 wt.%.

After the Hercynian period, sinistral strike–slip movement of the Xiaojiang and Zhaotong–Qujing faults formed NE-trending tectonic zones in NE Yunnan. These zones are largely composed of NE-trending folds and compressional-shear faults that are accompanied by NW-striking tensile faults that lie perpendicular to major structures, forming the sinistral "xi-type" tectonic Zn–

Table 5
Chemical compositions (wt.%) of ore-host rocks and altered rocks in the Huize Zn–Pb–(Ag) district, Yunnan, China

Sample number	Rock type	SiO_2	TiO_2	Al_2O_3	TFe	MnO	MgO	CaO	Na_2O	K_2O	P_2O_5	CO_2	IT	Σ
Sc-32	Dolomitic limestone	2.50	0.27	0.23	0.12	0.01	4.90	54.1	0.03	0.02	0.001	37.05	0.45	99.68
Sc-33	Coarse-crystalline dolomite	3.75	0.37	0.24	0.20	0.02	14.7	38.8	0.04	0.04	0.001	37.20	4.00	99.36
Sc-34	Coarse-crystalline dolomite	3.59	0.01	0.47	0.14	0.01	8.90	47.1	0.04	0.01	0.003	36.70	2.30	99.27
Sc-35	Coarse-crystalline dolomite	2.21	0.06	0.23	0.19	0.01	15.9	42.7	0.05	0.03	0.001	34.52	3.45	99.35
HR-5	Coarse-crystalline dolomite	4.85	0.21	0.23	0.92	0.01	15.1	34.9	0.04	0.04	0.001	37.30	5.60	99.20
HQ-89	Coarse-crystalline dolomite	5.39	0.001	1.65	0.38	0.01	17.8	34.2	0.05	0.16	0.001	34.8	4.90	99.34
HQ-173	Limestone	3.40	0.35	0.47	0.23	0.01	1.10	55.1	0.04	0.06	0.220	38.0	0.71	99.64
HQ-176	Coarse-crystalline dolomite	1.96	0.17	0.09	0.24	0.07	20.4	33.1	0.03	0.02	0.002	37.9	5.30	99.28
HQ-88	Mineralised-altered dolomitic limestone	9.44	0.35	2.83	1.50	0.02	7.20	41.7	0.05	0.82	0.002	33.7	1.60	99.21
HQ-175	Mineralised-altered dolomite	13.0	0.52	9.92	1.71	0.02	10.1	28.6	0.06	2.09	0.001	30.1	3.20	99.32
HQ-171	Mineralised-altered dolomite	11.6	0.30	5.20	2.07	0.02	8.40	38.3	0.05	0.64	0.001	31.2	1.60	99.38
HQ-172	Mineralised-altered dolomite	12.1	0.75	8.97	6.00	0.16	5.90	34.6	0.04	0.53	0.250	27.1	3.37	99.77

Analytical unit: Open Laboratory of Ore Deposit Geochemistry, Institute of Geochemistry, Chinese Academy of Sciences, P.R. China.
Contents of major chemical composition of the rocks were analysed by wet chemistry. TFe = Fe_2O_3 + FeO. The methods of sample processing are the same as Table 2.

Pb–(Ag) metallogenic region. The Huize Zn–Pb–(Ag) district is located in the Jinniushang–Kuangshanchang ore-controlling fault zone, in the southwestern segment of the Dongchuan–Zhenxiong NE-trending tectono-metallogenic zone. Medium- to large-sized Zn–Pb–(Ag) deposits and occurrences are present along the fault systems (Fig. 1).

The main ore-controlling structures of the district are the Kuangshanchang, Qilinchang and Yinchangpo faults. The tectonites of the fault zones contain hydrothermal alteration of dolomite, pyrite, silica, chlorite, epidote, and calcite. Adjacent wall rocks contain widespread carbonate veins and quartz veinlets, reflecting signs of fault-fluid activity. In addition, the fault tectonites contain anomalous concentrations of Pb, Zn, Fe, Ge, As, Ag, Tl and other trace elements, with Fe concentrations of about 18 wt.% and (Pb + Zn) contents of 0.7 wt.% (Table 6).

Local ore-controlling structures of the Kuangshanchang, Qilinchang and Yinchangpo deposits are fault-derived NE-striking compressional-shear zones and NW-extending tensile faults. The NE-striking faults (the major ore-hosting structures) are restricted to orebodies within the middle and upper horizons of the Baizuo Formation, defining the hanging wall and footwall of the orebodies. Joints and fractures derived from these structures control veinlet mineralisation. In addition, these structures control parallel ore veins where rock layers abruptly change their attitude near the faults. The strata-bound and lenticular orebodies are generally coincident with the attitudes of the country rocks

Table 6
Metal contents in fault tectonites in the Huize district, Yunnan, China

Sample number	Fault	TFe	Cu	Zn	Ga	Ge	As	Mo	Ag	Cd	In	Sb	Tl	Pb
DC-17	1	na	57.0	217.4	34.9	3.5	na	1.4	na	0.3	0.1	6.0	1.5	76.6
HQC-2	2	6.8	79.6	119.2	10.6	1.4	32.9	1.8	0.2	0.3	0.1	3.4	0.4	30.6
HQC-125	2	0.9	4.5	607.7	0.5	0.4	10.6	0.3	6.0	1.5	0.0	12.3	0.2	6,725.0
HQC-7	3	5.2	12.2	324.0	6.0	2.8	268.9	2.9	0.4	0.4	0.0	2.4	0.5	162.5
HQC-9	3	11.4	39.5	537.3	17.9	1.9	32.9	2.1	0.3	0.8	0.1	2.2	1.5	111.8
HQC-14	3	18.8	97.4	216.0	19.2	3.0	346.4	6.5	0.3	0.8	0.1	38.8	1.0	67.2
HQC-97	4	0.9	5.4	1,845.0	1.4	0.3	113.3	2.9	22.4	2.1	0.0	7.2	0.1	675.0
HQC-171	5	2.5	14.8	1,197.0	5.2	0.8	26.0	0.7	0.4	3.6	0.0	11.1	0.3	317.3
HQC-29	5	1.1	2.7	580.7	0.1	0.5	85.9	0.1	0.1	1.8	0.0	51.4	0.1	508.8
HQC-12	6	0.9	3.5	141.2	0.5	0.3	22.5	0.4	0.1	0.4	0.0	2.1	0.0	72.8

Analytical unit: Open Laboratory of Ore Deposit Geochemistry, Institute of Geochemistry, Chinese Academy of Sciences, P.R. China.
Contents of TFe (%) and Zn (>1%) were analysed by wet chemistry. TFe = Fe_2O_3 + FeO. Contents of trace elements (ppm) by ICP-MS techniques; analytical method, detection limits of elements (ppm), standard samples and the method of sample processing are the same as Table 3.
1, Xiaojiang Fault; 2, Qilinchang Fault; 3, Kuangshanchang Fault; 4, NE-trending Fault; 5, NW-trending Fault; 6, NS-trending Fault. na, not analysed.

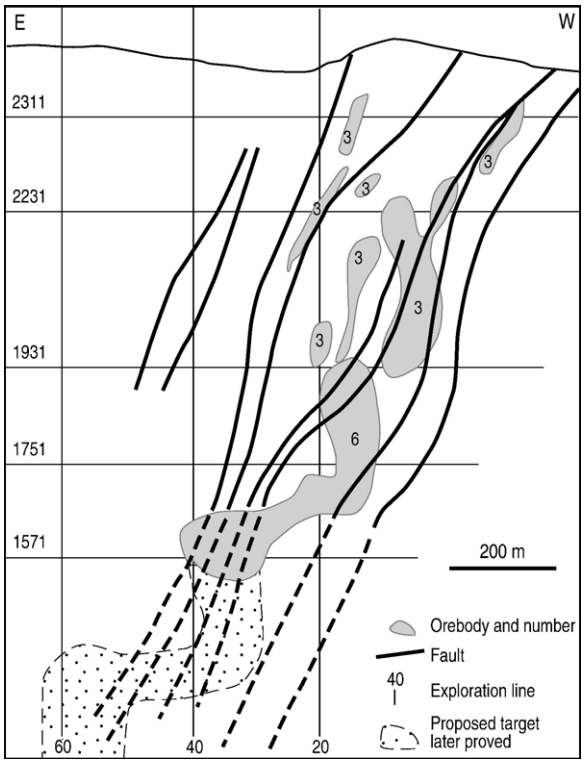

Fig. 8. E–W cross-section of the Qilinchang deposit showing outline of the orebody, Huize Zn–Pb–(Ag) district, Yunnan, China.

(Fig. 4). The NW-striking faults developed along the hanging wall of the ore-conduits and tend to decrease in fracture density from shallow to deeper levels, increasing in size at depth. These faults, linked with the Qilinchang ore-conduit fault, control the geometrical distribution of the ore deposits. Although orebodies are not known along the linking faults, hydrothermal alteration and sub-economic Zn–Pb–(Ag) mineralisation in the tectonites within them stand out from those in the NS-striking faults; the tectonites contain as much as 0.15 wt. % (Pb+ Zn) (Table 6). At junctions between NW- and NE-striking faults, the orebodies expand locally, reflecting the ore-controlling nature of the intersections (bonanza ores).

Ore-controlling structural types in the Huize Zn–Pb–(Ag) district are both "terraced" and "xi-type" structures (Han et al., 2001c). The "xi-type" ore-controlling structures are spatially associated with orebodies that are distributed along a set of compressional shear zones. These shear zones, together with the NW-striking tensile faults, constitute the "xi-type" ore-controlling structures which are typical ore-controlling structures at both the district and regional scale. The Qilinchang, Kuangshanchang and Yinchangpo faults constitute an imbricate structure (see Fig. 2), which controls the Kuangshanchang, Qilinchang and Yinchangpo deposits, giving rise to three distinct Zn–Pb–(Ag) ore zones.

Examples of "terraced-type" ore-controlling structures are present in the Qilinchang Zn–Pb–(Ag) deposit and are spatially coincident with the Qilinchang fault-derived NE-striking compressional shear zones and the NW-striking tensile faults. The orebodies are localised along the same intervals in both horizontal and vertical directions, as viewed both in plan and in cross-section. Metallo-tectonic controlling systems are characterised by ore-controlling structures of different scales in the region such as district-scale and orebody-scale structures. The NE-trending tectonic zone is the most important metallogenic system in the district and is defined as follows:

(1) The Sichuan–Yunnan–Sichuan Zn–Pb–(Ag) metallogenic region includes Zn–Pb–(Ag) deposits and lesser occurrences distributed within five sinistral Zn–Pb–(Ag) tectono-metallogenic zones: (a) Xundian–Xuanwei; (b) Dongchuan–Zhenxiong; (c) Huize–Yiliang; (d) Ludian–Yanjin; and (e) Yongshan–Suijiang zones (Fig. 1),

which constitute the "xi-type" structural system in NE Yunnan;
(2) The Kuangshanchang, Qilinchang and Yinchangpo deposits are developed in a sinistral en echelon pattern, forming the high-grade "xi-type" structures of the Huize Zn–Pb–(Ag) district (Fig. 2);
(3) The Nos. 3, 6, 8 and 10 orebodies constitute second-order "xi-type" structures of the Qilinchang deposit. This is the result of sinistral torsion of the Qilinchang fault;
(4) The orebodies and geochemical anomalies form an en echelon array and are distributed in the NE compressional shear zone (Han et al., 2001b), where orebodies are strictly controlled by "terraced-type" structures, showing a characteristic orebody plunge to southwest (Fig. 8).

6.2. Lithological control

Lithological influences on the location and shape of orebodies in the shear zones are evident through the petrogeochemical contrasts between the coarse-crystalline dolomite and the silicified dolomitic limestone of the Baizuo Formation (Fig. 5C and D). Although previous workers suggested that the Huize Zn–Pb–(Ag) district was directly controlled by formation of the Baizuo Formation, there are reasons why this cannot have been the case. Since the coarse-crystalline dolomite in the middle and upper horizons of the Baizuo Formation is relatively thick (50–80 m), it contains a highly effective porosity and its mechanical properties (compression-resisting strength and shear-strength) are poorer than those of the underlying silicified dolomitic limestone. Therefore, rock failure under the tectonic stress field took place preferentially along the weak contact planes and rock layers (bedding and lithological boundaries) such as the boundaries between the coarse-crystalline dolomite and the underlying silicified dolomitic limestone; these planes subsequently developed into large-scale faults and fractures.

Brecciation and fragmentation in the fault zone would have provided channels and space that would have created favourable conditions for circulation of ore-fluids to form "stratabound" and lenticular orebodies. In addition, the silicified dolomitic limestone, which has a relatively low effective porosity, together with the Early Permian Liangshan Formation coal series strata, would have shielded and protected the ore horizon as a physical and chemical seal. Furthermore, the coarse-crystalline dolomite in the middle and upper parts of the Baizuo Formation are chemically active and are intercalated with structurally weak evaporite, thus forming an additional geochemically reactive zone.

It is also noteworthy that evaporite layers are present in the host rocks and in the underlying strata of the Early Sinian Dengying Formation and Early Cambrian Qiongzhushi Formation (Liu and Lin, 1999). Evaporite layers are also present in the middle and lower parts of the Baizuo Formation; X-ray diffraction indicates they are mainly composed of gypsum, barite and other minerals.

7. Geochemical characteristics of the deposits

Isotopic studies (S, Pb, C, O, and Sr) were undertaken on the Zn–Pb–(Ag) ores and on associated rocks and minerals in order to support genetic models which are compatible with the field and microscopic observations. The isotopic studies were coupled with fluid-inclusion investigations to better define the characteristics of the ore fluid and its depositional environment.

7.1. Isotope geochemistry

The sulphur isotopic composition (Table 7) of sphalerite, galena, pyrite and gypsum is generally similar to that of global Carboniferous seawater sulphate (15–20‰; Claypool et al., 1980), suggesting that sulphur in the ore was derived predominantly from evaporite rocks in the strata.

The lead isotopic composition of ore minerals is homogeneous: $^{206}Pb/^{204}Pb = 18.251–18.496$, $^{207}Pb/^{204}Pb = 15.663–15.855$, $^{208}Pb/^{204}Pb = 38.487–39.0$, similar to that of basalts in the region: $^{206}Pb/^{204}Pb = 18.175–18.371$, $^{207}Pb/^{204}Pb = 15.629–15.662$, $^{208}Pb^{204}Pb = 38.38–38.666$. It differs significantly, however, from the dolomite that hosts the ore: $^{206}Pb/^{204}Pb = 18.482–18.673$, $^{207}Pb/^{204}Pb = 15.791–15.963$, $^{208}Pb^{204}Pb = 39.124–39.685$ (Table 8). These data (Fig. 9) clearly show that Pb in the ore fluid was a mixture of upper crustal Pb and orogenic-belt Pb.

The C and O isotopic composition of gangue calcite may shed light on the nature of the ore fluid (Table 9). In combination with the lithological environment of ore deposition, it was deduced that the ore-forming fluids were derived from mixed sources, involving metal-rich fluids circulating in the basement and cover rocks, and deep-sourced fluids related to metamorphic dewatering at depth. The C and O isotopic composition of calcite ($\delta^{13}C_{PDB}$: −1.2‰ to −3.3‰, $\delta^{18}O_{SMOW}$: 11.31‰ to 20.89‰) is different from that of the ore-hosting dolomite ($\delta^{13}C_{PDB}$: −3.35‰ to 0.85‰, $\delta^{18}O_{SMOW}$: 11.31‰ to 16.95‰) (Table 9) and therefore was probably derived from a deep source region ($\delta^{13}C_{PDB}$: −4‰ to −10‰; Zhang, 1995). The $\delta^{13}C$ and $\delta^{18}O$ values progressively decrease from unaltered to Zn–Pb–(Ag)

Table 7
Sulphur isotopic composition of sulphides from the Huize Zn–Pb–(Ag) district, Yunnan, China

Number	Sample number	Mineral	$\delta^{34}S$ (‰CDT)	$\pm\sigma$ (‰)	Location
	LTB-2-1[a]		1.895	0.011	
	LTB-2-2[a]		1.981	0.025	
1	1571-8	Py	15.75	0.019	No. 6 orebody at level 1571 in Qilinchang deposit
2	1571-11	Sp	11.8	0.030	
3	HQ-84	Ga	12.04	0.016	
4	1631-7-1	Sp	14.22	0.038	No. 6 orebody at level 1631 in Qilinchang deposit
5	1631-7-2	Sp	14.32	0.031	
6	1631-7-3	Sp	13.98	0.021	
7	HQ99-1	Py	10.63	0.014	
8	C_2W	Py	15.81	0.017	Ore-host Dolomite of No. 6 orebody in Qilinchang deposit
9	Qilinchang-1	Gy	13.97	0.02	Dolomite of the periphery of the district
10	No. 8	Gy	17.59	0.02	
11	HQ-485	Py	15.73	0.036	No. 8 orebody in Qilinchang deposit
12	HQ-490	Py	15.12	0.006	
13	HQ-493X	Py	14.21	0.048	
14	HQ-495	Py	15.25	0.033	
15	HQ-498	Sp	13.37	0.018	
16	HQ-487	Sp	23.49	0.01	
17	HQ-495	Sp	12.66	0.041	
18	HQ-491	Sp	14.92	0.032	
19	HQ-491	Ga	14.82	0.013	
20	HQ-495	Ga	10.87	0.026	
21	HQ-503X	Py	15.47	0.048	Ore-host Dolomite of No. 8 orebody in Qilinchang deposit
22	HQ-473C	Py	5.72	0.028	
23	MQ-912	Py	11.80	0.038	Orebody No. 1 in Kuangshanchang deposit
24	MQ-909S	Sp	13.32	0.04	
25	MQ-911	Sp	13.20	0.011	
26	MQ-918Q	Sp	13.59	0.032	
27	MQ-915S	Sp	13.88	0.042	
28	MQ-910	Sp	13.02	0.038	
29	MQ-909Q	Sp	13.31	0.028	
30	MQ-911	Ga	11.77	0.017	
31	MQ-910	Ga	11.15	0.039	
32	MQ-918	Ga	11.40	0.012	
33	MQ-909	Ga	15.94	0.042	
34	MQ-1053	Py	3.16	0.041	Ore-host dolomite of Orebody No. 1 in Kuangshanchnag deposit

Analytical unit: No. 1–8 samples in Yichang Institute of Geology and Mineral Resources, Chinese Academy of Geological Sciences; No. 9–33 samples in Open Laboratory of Ore Deposit Geochemistry, Institute of Geochemistry, Chinese Academy of Sciences, P.R. China. All samples analysed by SO_2 method. Py, pyrite; Sp, sphalerite; Ga, galena; Gy, gypsum. Data of No. 8 sample from Liu and Lin (1999).
[a] Standard samples (LTB-2-1; LTB-2-2).

mineralised dolomite to calcite in both the Qilinchang and Yinchangpo deposits (Fig. 10). Carbon in the calcite was derived from a mixture of crustal carbon in the cover rocks and from deep-sourced carbon from the basement.

$^{87}Sr/^{86}Sr$ values of sulphide ores from the Qilingchang Zn–Pb–(Ag) deposit area range between 0.71021 and 0.71768; the average $^{87}Sr/^{86}Sr$ of 7 samples is 0.7114 (Han et al., 2003). Earlier, Zhou (1996) gave $^{87}Sr/^{86}Sr$ data for sulphide and gangue minerals from Qilingchang that fell between 0.70832 and 0.71808. In the Yinchangpo deposit, Hu (1999) found that the Baizuo Formation dolomite, gangue minerals (calcite) and ores show differences in $^{87}Sr/^{86}Sr$ ratios. The minimum $^{87}Sr/^{86}Sr$ value for dolomite (0.70868–0.7093) is close to the $^{87}Sr/^{86}Sr$ ratio of contemporaneous Carboniferous seawater (0.708–0.709); the $^{87}Sr/^{86}Sr$ ratio of sulphide ore is 0.71084–0.71877 and calcite values range between 0.72227 and 0.72557. The $^{87}Sr/^{86}Sr$ values of sulphide ore and calcite from the two deposits should represent those at the time of interaction between ore fluid and wall rocks during ore deposition. They are, however, higher than either those of the wall rocks and the contemporaneous seawater, suggesting that the ore fluid passed through a radiogenic Sr-source region.

Table 8
Pb isotopic composition of minerals and rocks from the Huize Zn–Pb–(Ag) district, Yunnan, China

Sample number	Mineral	$^{206}Pb/^{204}Pb$	$^{207}Pb/^{204}Pb$	$^{208}Pb/^{204}Pb$	Locality	Reference
1571-11	Sp	18.339±0.020	15.676±0.002	38.753±0.011	No. 6 orebody at level 1571 in Qilinchang deposit	1
1571-8	Py	18.393±0.034	15.688±0.006	38.820±0.020		
HQ-84	Ga	18.496±0.001	15.750±0.001	39.001±0.002		
1631-7-1	Sp	18.385±0.004	15.676±0.005	38.771±0.016	No. 6 orebody at level 1631 in Qilinchang deposit	
1631-7-2	Sp	18.441±0.005	15.679±0.005	38.772±0.020		
1631-7-3	Sp	18.353±0.020	15.663±0.001	38.719±0.001		
HQ99-1	Py	18.464±0.007	15.696±0.011	38.828±0.032		
44-5	Ga	18.436	15.683	38.861	No. 6 orebody at level 1571 in Qilinchang deposit	2
4-23	Ga	18.469	15.701	38.850		
44-5	Sp	18.487	15.72	38.874		
38-3	Ga	18.471	15.702	38.847	No. 6 orebody at level 1884 in Qilinchang deposit	
13-55	Ga	18.461	15.701	38.857	No. 6 orebody at level 1691 in Qilinchang deposit	
13-61	Ga	18.450	15.692	38.823		
13-24+1	Ga	18.474	15.701	38.844		
6-10	Ga	18.454	15.691	38.820	No. 6 orebody at level 1648 in Qilinchang deposit	
2014-1-11	Ga	18.469	15.700	38.850	No. 6 orebody at level 1631 in Qilinchang deposit	
2014-1-12	Ga	18.471	15.709	38.839		
2014-2-11	Ga	18.434	15.672	38.749		
2014-2-8	Ga	18.458	15.69	38.817		
2014-3-4	Py	18.474	15.700	38.845		
2014-2-8	Sp	18.455	15.694	38.814		
F-126	Sp	18.458	15.694	38.814	No. 6 orebody in Qilinchang deposit	
F-1	Sp	18.455	15.709	38.859		
F-135	Sp	18.462	15.713	38.874		
YC7P-6	Ga	19.073	16.334	40.695	Yichangpo deposit	3
YC6-23	Ga	18.645	15.866	39.368		
YC6-21	Ga	18.487	15.712	38.883		
YC7P-7	Ga	18.648	15.891	39.451		
YC6-25	Ga	18.314	15.576	38.513		
YC3-1K	f-ore	18.626	15.887	39.522		
YC3T-4	f-ore	18.542	15.798	39.167		
YC3-5K	Y-ore	18.439	15.716	38.955		
180-3	Ga	18.12	15.500	38.360	Pit 510 in Yinchangpo deposit	4
83-2	Ga	18.401	15.597	38.644	Pit PD6 in Yinchangpo deposit	
83-5	Ga	18.404	15.608	38.700	Yinchangpo deposit	
I80-2	Ga	18.13	15.440	38.420	Pit 510 in Yinchangpo deposit	
C-1	Ga	18.28	15.530	38.720	No. 7-1 Orebody in Kuangshanchang deposit	4
C-2	Ga	18.18	15.420	38.390	No. 6-1 orebody in Kuangshanchang deposit	
I80-4	Ga	18.22	15.630	38.680	Pit 405 in Kuangshanchang deposit	
I80-5	Ga	18.22	15.630	38.670	Pit 529 in Kuangshanchang deposit	
F-5	Dm	18.54	15.899	39.562	Kuangshanchang (D_3z)	2
S5-1	Dm	18.482	15.784	39.142	Kuangshanchang (Zbd)	
SO-1	Bas	18.371	15.662	38.666	District (P_2â)	2
SO-2	Bas	18.175	15.629	38.380	District (P_2â)	
F-4	Dm	18.51	15.791	39.124	District (C_1b)	
14-2-12	Dm	18.673	15.963	39.685	Qilinchang (C_1b)	

References: 1, this paper, analysed at Yichang Institute of Geology and Mineral Resources, Chinese Academy of Geological Sciences, China; 2, Zhou (1996); 3, Hu (1999); 4, Liu (1996). Py, pyrite; Sp, sphalerite; Ga, galena; Dm, dolomite; Bas, basalt; F, ore-sulphide ore; Y, ore-oxide ore.

Regional geological conditions are compatible with supply of a radiogenic ore fluid either from Kunyang Group basement, containing high $^{87}Sr/^{86}Sr$ values, or from plutonic intrusions. Kunyang Group domomite has a $^{87}Sr/^{86}Sr$ ratio of 0.7281 (Chen, 1993b). During ascent, the ore fluid may have reacted with carbonate minerals in the Phanerozoic cover rocks (water/rock interaction), leading to significant differences in Sr isotopic composition of the wall rock, ore, and gangue calcite. Because the Sr isotopic composition of galena ($^{87}Sr/^{86}Sr$=0.71092–0.71451) and sphalerite ($^{87}Sr/^{86}Sr$=0.70808–0.71490) from the Qilinchang deposit

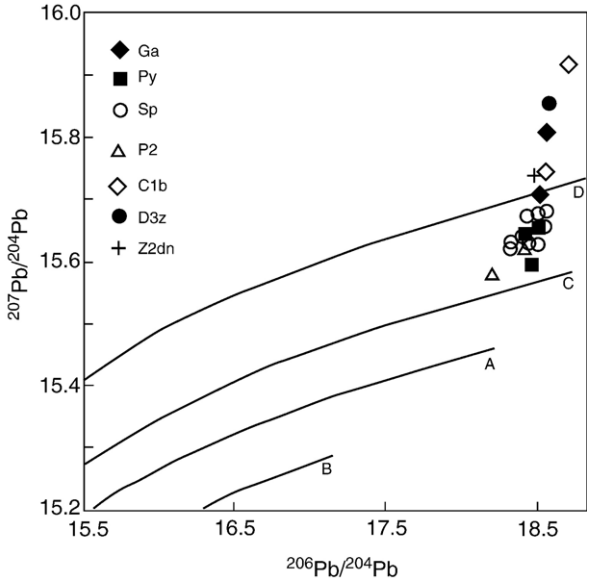

Fig. 9. Plumbotectonic plot of the Huize Zn–Pb–(Ag) deposits (after Zartman and Doe, 1981). P_2–Permian basalt, Z2dn–Late Sinian Dengying Formation, D3z–Devonian Zaige Formation, C_1b–Carboniferous Baizuo Formation; A–mantle, B–lower crust, C–orogenic belt, D–upper crust; Py, pyrite; Sp, sphalerite; Ga, galena.

(Li et al., 2000) is lower than that of the regional rocks, Li et al. (2000) considered that the Sr could not have come from the wall rock hosting the ore. There is, however, no obvious evidence for derivation of Pb, Zn and other ore-forming elements from the surrounding country rocks (Huang et al., 2001), especially since the Early Sinian igneous suite is absent in the Huize district. It is therefore proposed that the major part of Sr in the Huize deposits was derived from the Kunyang Group basement rocks.

7.2. Review of fluid inclusion data

Fluid inclusion characteristics of the Huize deposits are summarized herein, based on the senior author's own data and that of previous researchers. Fluid inclusions are present in calcite in large quantities. Two types of inclusions can be distinguished: (1) liquid only (L) inclusions and (2) liquid–vapour (L-V) inclusions. The inclusions are generally small (1–10 μm in size).

Single-phase brine liquid-only (L) inclusions from the Qilinchang and the Kuangshanchang deposits are relatively small, mostly around 6–10 μm, whereas those from the Yinchangpo deposit are relatively large, mostly around 3–20 μm, locally as much as 40 μm in size (Hu, 1999). The inclusions mainly have negative crystal, water-droplet, oval or rounded forms. A small sub-population is irregular in shape, spreading in clusters along the crystal planes of calcite.

In liquid–vapour (L-V) inclusions, the ratio of gas to liquid is 5–20%. Microthermometric data are given in Table 10. Morphology of the fluid inclusions is dominated by negative crystal form and water-droplet shape, a smaller population of inclusions is oval, rounded or irregular in shape. Fluid inclusions in the Qilinchang and the Kuangshanchang deposits are usually around 1–10 μm in size, whereas those from Yinchangpo are relatively larger, mostly around 3–20 μm but locally as large as 55 μm in size (Hu, 1999). The L-V inclusions make up 60–70% of the total population.

The liquid components of fluid inclusions in hydrothermal calcite from the ore-forming stage contain high concentrations of Na^+, Ca^{2+}, F^- and Cl^-, with $Na^+ > K^+$, $Ca^{2+} > Mg^{2+}$ and $Cl^- > F^-$; gaseous components are dominated by H_2O, CO_2, CO, CH_4 and H_2. The ore-forming fluid has moderate salinities (6–12 wt. % NaCl equiv.), low to moderate homogenisation temperatures (165–220 °C) and pressure in the range 4.1–6.6 MPa (Table 10). According to Liu and Lin (1999), the fluid inclusions contain metallic elements such as Pb, Cu, Ba, Sr and Mn (Pb: 1.7–2.0 mg/l, Cu: 1.3–3.4 mg/l, Ba: 17.20–48.2 mg/l, Sr: 3.5–4.9 mg/l, Mn: 9.0–12.8 mg/l). Thus, the hydrothermal solutions are interpreted as metal-bearing Na–Ca–Cl brines.

8. Discussion—deposit genesis

Ores in the Huize deposits are present not only in the main ore-hosting strata, but also in ore-bearing faults, leading to the conclusion that the ore-hosting strata, ore-bearing faults, and orebodies are all interrelated. The geological features of the deposits are comparable to those of many MVT-type Zn–Pb–(Ag) deposits (Table 11). The principal similarities are tectonic setting, type of host rock, wall rock alteration style and mineral composition. Nevertheless, the Huize Zn–Pb–(Ag) deposits display a series of unique geological characteristics that contrast sharply with those of typical MVT Zn–Pb–(Ag) deposits. These include the distinct ore-controlling structure, lithological character, relationship to magmatic rocks, ore texture and structure, homogenisation temperatures of fluid inclusions, and the widespread presence of Ag and other trace elements in the ore.

The fluid inclusion and isotope geochemical data, as well as the tectonic ore-controlling characteristics (Han et al., 2001d) for the Huize Zn–Pb–(Ag) district indicate that ore-forming elements such as Pb, Zn, Ag, and Ge were predominantly derived from the Kunyang

Table 9
Carbon and oxygen isotopic composition of minerals and rocks in the Huize Zn–Pb–(Ag) district, Yunnan, China

Sample number	Mineral/rock	T_h[a] (°C)	$\delta^{13}C$ (‰ PDB)	$\delta^{18}O$ (‰ SMOW)	$\delta^{18}O$ (‰ PDB)	$\delta^{18}O$ (‰) (fluid)[b]	Locality	Reference
HQO-99-1	Calcite	193 (15)[c]	−1.94	17.088	−13.36	7.78	No. 6 orebody at level 1631 in Qilinchang deposit	1
HQO-109-4	Calcite	221 (15)	−3.27	17.789	−12.68	10.08		
1631-38	Calcite	164 (20)	−2.97	18.562	−11.93	7.78		
HQ-84	Calcite	208 (12)	−3.23	18.211	−12.27	9.7	No. 6 orebody at level 1631 in Qilinchang deposit	
HQ-109-4	Calcite	221 (15)	−3.31	17.789	−12.68	7.55		
1571-2	Calcite	172 (15)	−3.3	18.211	−12.27	7.7		
Hui-2-3	Calcite		−2.75	17.8	−12.67	7.14	No. 6 orebody at level 1751 in Qilinchang deposit	2
38-3	Calcite		−2.8	17.1	−13.4	6.44	No. 6 orebody at level 1884 in Qilinchang deposit	
Hui-6-10	Calcite		−2.9	17.8	−12.6	7.14	No. 6 orebody at level 1648 in Qilinchang deposit	
13-61	Calcite		−2.7	18.1	−12.4	7.44	No. 6 orebody at level 1691 in Qilinchang deposit	
Hui-1-1	Calcite		−3.2	18.43	−12.06	7.77	No. 6 orebody at level 1836 in Qilinchang deposit	
14-2-8	Calcite		−2.6	18.7	−11.8	8.04	No. 6 orebody at level 1631 in	
14-3-6	Calcite		−2.7	18.4	−12.1	7.74	Qilinchang deposit	
Hui-1-2	Near-ore-dolomite		0.77	21.6	−9.41			
Hui-5-1	Calcite		−2.4	18.1	−12.3	7.44	No. 6 orebody at level 1571 in	
Hui-4-23	Calcite		−3.1	17.5	−13	6.84	Qilinchang deposit	
23-4R	Calcite		−3	17.6	−12.8	6.94		
HQC-25	Barite-bearing Pb-Zn mineralised broken dolomite		0.3	20.4	−10.1			1
HQC-98	Pb–Zn mineralised dolomite cataclasite		−3.2	19.5	−11		No. 6 orebody at level 1631 in Qilinchang deposit	3
HQC-92	Pb–Zn mineralised dolomitic cataclasite		−1.6	17.8	−12.7			
14-3-19	Near-ore altered dolomite		−0.8	20.5	−10.1			
Hui-8	Barite	140	na	8.29	na	−2.05	Kuangshanchang deposit	2
HE16	Bioclastic irregular limestone		−0.44	22.45	−8.16		At level 2233 in Kuangshangchang deposit	4
HE18	Bioclastic irregular limestone		−1.5	21.33	−9.24			
HE17	Fine-medium-crystalline dolomite		0.85	20.98	−9.58			
ycp4-7	Calcite		−0.58	20.89	−13		Yichangpo deposit	5
ycp3-17	Calcite		−3.18	17.51	−12.95			
ycp5-8-c	Calcite		−2.23	13.23	−17.1			
ycp6-a	Calcite		−1.49	16	−13.49			
ycp6-1	Calcite		−2.16	12.97	−11.99			
ycp6-3	Calcite		−2.57	17.46	−18.96			
ycp2-a	Coarse-crystalline dolomite		0.75	20.99	−9.57			
ycp2-b	Coarse-crystalline dolomite		0.81	20.98	−9.58			
ycp3-lk	Medium-crystalline dolomite		−0.29	16.95	−9.67			
ycp3-5k	Bioclastic limestone		−2.32	18.5	−14.41			
SC-33	Dolomitic limestone		−0.9	21	−9.6		Sunjiagou in the periphery of the district	1
SC-34	Coarse-crystalline dolomite		−2.2	20.5	−10.1			
SC-35	Coarse-crystalline dolomite		−1.2	21.4	−9.2			

(continued on next page)

Table 9 (*continued*)

Sample number	Mineral/rock	T_h [a] (°C)	$\delta^{13}C$ (‰ PDB)	$\delta^{18}O$ (‰ SMOW)	$\delta^{18}O$ (‰ PDB)	$\delta^{18}O$ (‰) (fluid) [b]	Locality	Reference
HE11	Fine-medium-crystalline dolomite		0.85	19.32	−11.19		Zhujiayakou in the periphery of the district	4
HE10	Shell-bearing dolomitised limestone		−3.35	19.42	−11.1			
HE12	Shell-bearing dolomitised limestone		−1.1	20.09	−10.45			
HE02	Fine-medium-crystalline dolomite		0.09	22.6	−8.01		Qingchaojie in the periphery of the district	
HE01	Bioclastic irregular limestone		−1.15	22.59	−8.02			
HE03	Dolomitised limestone		−0.53	23.14	−7.49			

Analytical unit of this study: Isotope Laboratory of the Yichang Institute of Geology and Mineral Resources, Ministry of State Land Resources.
References: 1, this paper; 2, Liu and Lin (1999); 3, Zhou (1996); 4, S.J. Chen (1984); 5, Hu (1999).
[a] T_h=average homogenisation temperature.
[b] $\delta^{18}O_{H_2O}$ is calculated on the basis of $1000\ln\alpha_{\text{calcite-fluid}}=2.78\times10^6T^{-2}-2.89$ (O'Neil et al., 1969).
[c] Number of inclusions in parenthesis.

Group basement rocks, but were also partly derived from the evaporite-bearing cover rocks. The evaporate rock layers are believed to be closely related to the metallogenesis of the Huize ore district.

Following the Hercynian event, the Pacific Plate subducted from SE to NW, leading to sinistral strike slip movement of the Xiaojiang fault zone and Zhaotong–Qujing fault zones. The sinistral strike–slip movement led

Table 10
Homogenisation temperature and salinity of two-phase (liquid–vapour) fluid inclusions in calcite from the Huize Zn–Pb–(Ag) district, Yunnan, China

Sample number	Fluid inclusion type	Gas–liquid ratio (%)	Size (μm)	Feature of fluid inclusions	Homogenisation temperature (°C)		Salinity (wt.% NaCl equivalent)		Pressure (10^5 Pa)	Locality
					Range	Average	Range	Average		
1571-2	Liquid–vapour inclusion	5–10	1–5 1–8	Negative crystal, oval, rounded, and irregular form	168–232	172	6–10.8	9.0	543	Qilinchang
HQ-84	Liquid–vapour inclusion	5–20	1–8	Oval, irregular form with a small number of negative crystal form						
			1–10	Negative crystal form	189–240	208	6.3–9.0	7.6	572	
1631-1	Liquid–vapour inclusion	5–15	1–8 1–10	Rounded, oval and irregular forms with a small number of negative crystal form	142–205	164	5.5–8.5	7.0	463	
HQ109-4	Liquid–vapour inclusion	5–15	1–8 1–10	Negative crystal, oval and irregular form	203–245	221	5.7–10.5	8.8	618	
HQ-99-1	Liquid–vapour inclusion	5–10	1–8 1–10	Negative crystal, oval and irregular form	181–204	193	5.0–7.8	6.6	540	
44-1	Liquid–vapour inclusion	5–15	1–15 5–70	Irregular form as dominant type with a small number of negative crystal form	147–202	165	8–10.7	9.6	459	
MQ914	Liquid–vapour inclusion	5–20	1–10 3–15	Negative crystal/oval form as dominant type with a small number of irregular form	138–226	175	9.4–13.5	11	556	Kuangshanchang
MQ912	Liquid–vapour inclusion	5–30	1–10 3–12	Negative crystal, irregular, and oval form	198–240	217	6.8–16.0	12	661	

Analytical unit: Department of Geological Sciences, Kunming University of Science and Technology, P.R. China.
The heating/freezing equipment are T1350 heating stage, TRL-02 heating and cooling stage and KBL-1 cooling stage.

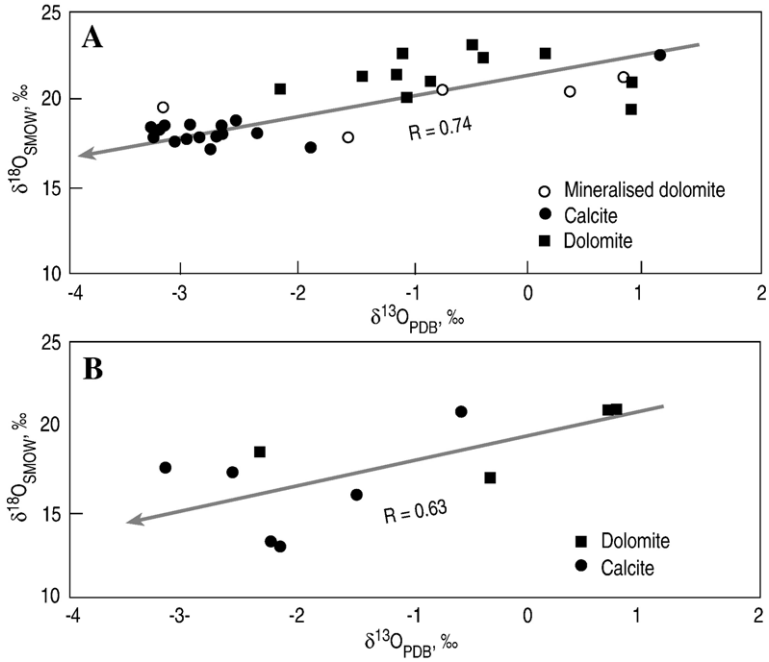

Fig. 10. $\delta^{13}C$ vs. $\delta^{18}O$ plot of the Qilinchang Zn–Pb–(Ag) deposit (A) and the Yinchangpo Zn–Pb–(Ag) deposit (B), the Huize Zn–Pb–(Ag) district, Yunnan, China.

to formation of five NE-trending tectono-metallogenic zones in northeastern Yunnan (from the south to the north). These zones are composed of NE-trending fold and compressional shear zones associated with the NW-trending tension or tensional faults, which, in turn, lie perpendicular to the main structure and form the "xi-type" structures. These tectonic zones are not only spatially coincident with regional magmatic activity, but also may have served as heat centres that localised development and distribution of the Zn–Pb–(Ag) deposits in the region. In addition, the strike–slip movement also led to the structural overlap of the NE-trending tectonic zone, creating the driving force for 'circulation' of deep-sourced fluids and consequently to mineralisation.

Ore-bearing fluids most likely entered the depositional environment during the period in which the host strata, together with the rest of the sequence, were being folded and deformed. This resulted in 'fluid circulation' along the ore structures. The fluids mixed with evaporites in the basement and the cover strata, extracting Pb, Zn, S and other ore-forming elements from the evaporites. The ore-forming fluids then moved along geochemical and pressure gradients into the NE-trending compressional shear zones (ore-hosting structures) in the highly porous, evaporite-bearing country rocks as they travelled away from the NW-striking faults (ore-distributing structures) and continuously dissolved the ore-forming materials along ore-host structures. Due to changes in physical and geochemical conditions, the ore minerals were precipitated to form the metallic sulphide-rich Zn–Pb–(Ag) deposits at Huize.

9. Conclusions

The Huize Zn–Pb–(Ag) deposits are comparable to MVT deposits in terms of tectonic setting, ore-host rock, wall-rock alteration, and mineral composition. However, the Huize Zn–Pb–(Ag) district is deformed and structurally controlled, and has ore-forming temperatures, Ag contents and associated trace minerals that are uncommon in many sedimentary-hosted MVT-type Zn–Pb–(Ag) deposits. Estimates of ore-forming temperatures of the Huize Zn–Pb–(Ag) deposits indicate a slightly higher temperature than those associated with MVT-type deposits (Table 11). Field and laboratory studies suggest that ore-forming materials were derived from the Kunyang Group basement rocks and the evaporite-bearing rocks of the cover strata. The Huize deposits formed from circulation of mixed ore fluids, together with the ore-forming elements, which were channelled along the ore-controlling structures.

Characterisation of the environment of ore formation in the Huize Zn–Pb–(Ag) district provides new constraints for ore genesis, as well as offering clues to the localisation of concealed carbonate-hosted Pb–Zn deposits in the deep interior of the district and its peripheries. The work also highlights the potential for discovery of similar deposits elsewhere in NE Yunnan Province, and indeed in the entire Sichuan–Yunnan–Guizhou Zn–Pb–(Ag) metallogenic region.

Acknowledgements

The senior author thanks the leaders and technicians of the Huize lead–zinc mine and its mining and exploration

Table 11
Comparison of major features of MVT Pb–Zn deposits and the Huize Zn–Pb–(Ag) deposits, Yunnan, China

Characteristics	MVT-type Pb–Zn deposits	Deposits in the Huize Zn–Pb–(Ag) district
Tectonic setting	On the margins of ancient cratons or in their interior or orogenic belts (Brannon et al., 1992; Eisenlohr et al., 1994; Titley, 1996); generally related with tectonic collision and/or rift activities (Christensen et al., 1995a,b).	In the southern part of the Northeast Yunnan depression basin in the Yunnan–Sichuan–Guizhou Pb–Zn metallogenic zone at the western margin of the Yangtze block, China. In the structurally composite position of the NE-, NS- and NW-extending tectonic zones situated on the Jinniuchang–Kuangshanchang tectonic zone in the southwestern segment of the Dongchuan–Zhenxiong NE-extending tectonic zone derived from the Xiaojiang fault zone and the Zhaotong–Qujing concealed deep fault zone; this region is considered as a concentrated hot-spot centre.
Deposit scale	Pb–Zn metal reserve of the main deposits 2.0–29.4 Mt. Some individual deposits are distributed over an area of 100 km^2.	The Pb–Zn metal reserves in Huize district are approximately 5 Mt; distributed within an area of about 20 km^2.
Ore-host wall rock	Occurring in Pt_2–T_3 sedimentary basin carbonate rocks (coarse-crystalline dolomite), the wall rocks mostly Pt_2 in age; some deposits occurring in the contact plane between carbonate rocks and clastic rocks.	Occurring in C_1b greyish-white, yellowish-red, cream-yellow coarse-crystalline dolomite and light-coloured lime dolomite; obvious rock-controlling characteristics.
Orebody feature	Horizontal orebodies distributed along faults or stratigraphic planes; veined, network and layered metasomatic orebodies.	Lenticular, stratifrom, veined and pocket-shaped orebodies occurring in the steeply sloppy interstratified compress-shear fault zone.
Rock facies and palaeogeography	Shallow environment in the basin on the margin of continental blocks.	Marginal environment of platform basins; the orefield located near the facies boundary of sedimentary or diagenetic origin.
Structure	Open space in carbonate rocks usually as the prerequisite for the formation of orebodies; folds and small faults as the major ore-controlling structures; paleokarst, sinks, dissolved collapse breccias and secondary fractures controlling the deposits (orebodies).	Ore deposits controlled by NS-, NE- and NW-extending faults, strictly controlled by structures; the NE-extending tectonic zone controlling the formation and enrichment of ore deposits.
Relation with magmatic rocks	Generally no genetic connection with magmatic rocks.	Late Hercynian basalts widespread in the orefield, with intrusive rocks occurring locally, their development close to Pb–Zn deposits (occurrences); in the vertical direction Pb–Zn deposits (occurrences) occurring in C_1b in the lower part of basalt unit.
Wall-rock alteration	Dolomitisation, jasperisation, clay alteration, pyritisation.	Dolomitisation, pyritisation, calcitisation being dominant; silicification and clay alteration seen locally.
Ore feature	Ores exhibiting disseminated and massive structures; sulphides exhibiting colloidal, skeleton coarse-crystalline textures; gangue minerals exhibiting coarse-crystalline textures; relatively low ore grade of most deposits: Zn: 5–7.2%; Pb: 0.5–4%; Zn>Pb for most deposit.	Mainly massive structure, disseminated structure less developed; ore minerals exhibiting fine-moderate-coarse-crystalline structures; high average ore grade: (Zn+Pb)>25–35%, Pb:Zn: 1:3–5 (excluding the Yinchangpo deposit).
Mineral composition	Sphalerite (low in iron), galena, marcasite, pyrite, dolomite, calcite commonly seen, with minor amounts of pyrrohotite, celestine, anhydrite, fluorite, barite, bitumen, etc.	Sphalerite, galena, pyrite, dolomite, calcite, marmatite commonly seen; with minor gypsum and barite; quartz, etc. seldom seen. Chalcopyrite commonly seen in Yinchangpo deposit.
Fluid inclusions	Ore-forming fluids being Na^+–K^+–Ca^{2+}–Cl^- type brines; homogenisation temperatures 50–175 °C; salinity 5–10 wt.% NaCl equiv.	Fluid inclusions dominated by liquid–vapour types, generally 5–25 μm in size; ore-forming fluid being of the Na^+–K^+–Ca^{2+}–Cl^-–F^-–SO_4^{2-} type; homogenisation temperature 164–221 °C; salinity 6.6–12 wt.% NaCl equiv.

(continued on next page)

Table 11 (*continued*)

Characteristics	MVT-type Pb–Zn deposits		Deposits in the Huize Zn–Pb–(Ag) district
Geochemical characteristics	Typical element	Major elements in the ore: Zn, Pb, Fe, Cu, Ba, F, Ca, Mg, Si, S, C, O. Ag in the ore: 4.7 ppm (Titley, 1993)	Major elements in the ore: Zn, Pb, Fe, S, Mg, Ca, C, O. Ores being enriched in Ag and dispersed elements (Table 3).
	Elements in major minerals	Sp: Fe (1–5%, up to 19.7% in individual cases), Pb, Cu, Ag (140 ppm), Cd, Ge, Mn, In, Co. Ga: Ag (40–60 ppm),Sb, Bi, Cu, Fe. Py: Co, Ni, Ag, Cu. Cc: Sr, Y, Ba, Mn.	SP: Fe, Pb, Ag (6.02–67.06 ppm), Cd, Ge, Ga, In, AS, Sb, Cu, Bi, Mn, Hg. Ga: Zn, Ag (75.84–144.5 ppm), Ga, As, Sb, Cu, Fe, Bi, MN. Py: Pb, Zn, AG (1.1–17.14 ppm), Tl, As, Sb, Cu, Co, Ni, Bi, Mo, Mn. Cc: Tl, Ga, Sr, Ba, Mn.
	Isotopic composition	Wide sulphur isotopic composition range (10–25‰); S derived mainly from seawater evaporate rocks; wide Pb isotopic composition range, generally J-type Pb-enriched (Sverjensky, 1986); The Pine Point deposit containing no radiogenic lead.	Sulphur isotopic composition: $\delta^{34}S$ generally within range of 6.3–17.75‰; S derived principally from evaporite rocks in the strata; Pb isotopic composition indicative of normal lead.

The main features of MVT Pb–Zn deposit are mainly based and compiled data from Kyle (1981), Titley (1993, 1996), Sverjensky (1986), Brannon et al. (1992), Eisenlohr et al. (1994), and Christensen et al. (1995a,b). Py, pyrite; Sp, sphalerite; Ga, galena; Cc, calcite.

staff for their excellent support and coordination. Thanks are due to Prof. Wang Xuekun of the Kunming University of Science and Technology, Senior Engineer Zhang Yifei of the Yunnan Provincial Bureau of Geology and Mineral Resources, and academicians Chen Qingxuan and Zhe Yusheng, Chinese Academy of Sciences, for their cordial instructions and suggestions. Especially, we thank Richard Kyle, Cameron Allen, and Spencer Titley for official reviews of the paper and their valuable suggestions and comments to improve the manuscript. The authors are indebted to Stephen Peters and Khin Zaw who dedicated much effort and time to provide relevant information and detailed comments for the revision of this manuscript but the interpretations made in this paper nevertheless remain the sole responsibility of the authors. This research project was granted jointly by the funds for 'Fostering Medium-aged and Young Academic and Technical Pioneers' (the Natural Science Foundation of Yunnan Province, No. 99D0003G), the National Natural Science Foundation of China (No. 40172038), the Nation State Climbing Project (No. 95-pre-39), supported by the Program for New Century Excellent Talents in University (NCET-04-917) and the Collaboration Program sponsored by the colleges and universities of Yunnan Province (No. 2000YK-04).

References

Brannon, J.C., Podosek, F.A., Mclinmans, R.K., 1992. A Qlleghenian age of the Upper Mississippi Valley-type zinc–lead deposit determined by Rb–Sr dating of sphalerite. Nature 356, 509–511.

Chen, H.S., 1993a. Isotope Geochemistry Research. Hangzhou. Zejiang University Publishing House. 38 pp. (in Chinese with English abstract).

Chen, J., 1993b. A discussion on the genesis and metallogenic model of the Qilinchang Zn–Pb–(Ag) sulfide deposit. Journal of Non-ferrous Mineral Resources and Exploration 2, 85–90 (in Chinese with English abstract).

Chen, S.J., 1984. A discussion on the sedimentary origin of Pb–Zn deposits in western Guizhou and northeastern Yunnan. Journal of Guizhou Geology 8 (3), 35–39 (in Chinese with English abstract).

Christensen, J.N., Halliday, A.N., Vearncomble, J.R., Kesler, S.E., 1995a. Testing models of crustal fluid flow using direct dating of sulfides: Rb–Sr evidence for early dewatering and formation of Mississippi Valley-type deposits, Canning Basin, Australia. Economic Geology 90, 877–884.

Christensen, J.N., Halliday, A.N., Leigh, K.E., Randell, R.N., Kesler, S.E., 1995b. Direct dating of sulfides by Rb–Sr: a critical test using the Polaris Mississippi Valley type Zn–Pb deposit. Geochimica et Cosmochimica Acta 59, 5191–5197.

Claypool, G.E., Holser, W.T., Kaplan, I.R., Sakai, H., Zak, I., 1980. The age curves of sulfur and oxygen isotopes in marine sulfate and their mutual interpretation. Chemical Geology 28, 190–260.

Compiling Committee of the Discovery History of Ore Deposits in China, 1998. The Discovery History of Ore Deposits in China (Volume of Yunnan). Geological Publishing House, Beijing, pp. 88–90 (in Chinese).

Eisenlohr, B.N., Tompkins, L.A., Cathles, L.M., Barley, M.E., Groves, D.L., 1994. Mississippi Valley type Zn–Pb deposits: products of brine expulsion by eustatically induced hydrocarbon generation? an example from northwestern Australia. Geology 22, 315–318.

Han, R.S., Sun, J.C., Gu, X.C., Li, J., Ma, G.S., Ma, D.Y., 1999. Metallogenic dynamics of the Yimen-type copper deposits and prognosis of concealed ores. Chinese Science Bulletin 44 (Suppl. 2), 250–252.

Han, R.S., Liu, C.Q., Sun, K.X., Ma, D.Y., Li, Y., 2000. Composite poly-genesis of Yimen-type copper deposit. Geotectonics and Metallogenesis 24 (2), 146–154 (in Chinese with English abstract).

Han, R.S., Chen, J., Li, Y., Gao, D.R., Ma, D.Y., 2001a. Discovery of concealed No.8 orebody at Qilinchang lead–zinc deposit in Huize mine, Yunnan. Geology–Geochemistry 29 (3), 191–195 (in Chinese with English abstract).

Han, R.S., Chen, J., Li, Y., Ma, D.Y., Ma, G.S., 2001b. Fault tectono-geochemical characteristics of the Qilinchang Pb–Zn deposit at Huize, Yunnan and localisation prognosis of concealed ores.

Acta Mineralogica Sinica 21 (4), 667–673 (in Chinese with English abstract).
Han, R.S., Liu, C.Q., Huang, Z.L., Chen, J., Ma, D.Y., Li, Y., 2001c. Study on the metallogenic model of the Huize Pb–Zn deposit in Yunnan Province. Acta Mineralogica Sinica 21, 674–680 (in Chinese with English abstract).
Han, R.S., Chen, J., Li, Y., Ma, D.Y., Zhao, D.S., 2001d. Ore-controlling tectonics and prognosis of concealed ores in the Huize Pb–Zn deposit, Yunnan. Acta Mineralogica Sinica 21 (2), 265–269 (in Chinese with English abstract).
Han, R.S., Liu, C.Q., Huang, Z.L., 2003. Rb–Sr isotope evidence for sources of ore-forming fluid in the Huize Zn–Pb–(Ag) district, Yunnan, China. Geochemica et Cosmochimica Acta (Suppl. A132).
Hu, Y.G., 1999. Occurrence of silver, sources of mineralized substances and ore-forming mechanism of Yinchangpo silver–polymetallic deposit, Guizhou Province, China. Unpublished Ph.D. Thesis, Institute of Geochemistry, Chinese Academy of Sciences, Guiyang, China, 67 pp. (in Chinese with English abstract).
Huang, Z.L., Han, R.S., Chen, J., Li, W.P., Xu, C., 2001. Ore-forming element contents of the periphery strata of the Huize Pb–Zn mine and Emeishan basalts and their significance. In: Hu, R.Z., Bi, X.W. (Eds.), Annual Report of the Open Lab. of Ore Deposit Geochemistry, Chinese Academy of Sciences. Guizhou Science and Technology Publishing House, Guiyang, pp. 99–103 (in Chinese with English abstract).
Kang, Y.T., 1982. Structures and metallogenesis at depths east of Honghe, Yunnan. Yunnan Geology 1 (1), 17–28 (in Chinese).
Korotev, R.L., 1996. A self-consistent compilation of elemental concentration data for 93 geochemical reference samples. Geostandards Newsletter 20, 217–245.
Kyle, R.J., 1981. Geology of the pine point lead–zinc district. In: Wolf, K.H. (Ed.), Handbook of Stratabound and Stratiform Ore Deposits, vol. 9. Elsevier Publishing Company, New York, pp. 643–741.
Li, C.Y., Tan, Y.J., Liu, Y.P., 2000. The prospective regions of Au, Pb–Zn and Sn at the southwestern and northwestern margins of the Yangtze block. In: Tu, G., Gao, Z., Li, C., Hu, R. (Eds.), Superlarge Ore Deposits in China (I). Science Press, Beijing, pp. 372–386 (in Chinese with English abstract).
Liao, W., 1977. A preliminary discussion on the genesis of the Kuangshanchang Pb–Zn deposit. A Geological Report of a Geological Part on the Huize Zn–Pb–(Ag) Mine from Bureau of Yunnan Geological and Mineral Resources Survey, China. 85 pp., (in Chinese).
Liao, W., 1984. A discussion on the S and Pb isotopic composition characteristics and metallogenic model of the Pb–Zn ore zones in eastern Yunnan and western Guizhou. Journal of Geology and Exploration 1, 1–6 (in Chinese with English abstract).
Liu, H.C., 1996. Zn–Pb–(Ag) source beds (rocks) in the Yunnan, Sichuan and Guizhou metallogenic provinces. Journal of Geology and Exploration 32 (2), 12–18 (in Chinese with English abstract).
Liu, H.C., Lin, W.D., 1999. Metallogenic rules of Zn–Pb– (Ag) deposits in northeastern Yunnan. Yunnan University Publishing House, Kunming, p. 39–47 and 307–317 (in Chinese).
Luo, X., 2000. A great breakthrough made in the prognosis of concealed ores in the deep interior of Huize Pb–Zn deposit—the newly proven reserves of Pb and Zn reached almost 1 million tonnes, its potential economic benefits will be several billion Chinese Yuan. Yunnan Daily A1 (18112) (in Chinese).
Luo, X., 2001. The Huize Pb–Zn deposit—a possible worldwide-known super-large deposit. Yunnan Daily A1 (18349) (in Chinese).
O'Neil, J.R., Clayton, R.N., Mayeda, T.K., 1969. Oxygen isotope fractionation in divalent metal carbonates. Journal of Chemistry and Physics 51, 5547–5558.
Qi, L., Hu, J.D., Conrad, G., 2000. Determination of trace elements in granites by inductively coupled plasma mass spectrometry. Talanta 51, 507–513.
Shao, S.C., 1995. Geology and geochemistry of the strata-bound Pb–Zn deposits at the western margin of the Yangtze block, Guiyang. Post-doctoral dissertation, p. 39–61 (in Chinese with English abstract).
Shen, S., 1988. The metallogenic rule ore-search orientation of the major ore resources at the Xichang–Middle Yunnan area. Chongqing Publishing House, Chongqing, pp. 78–123 (in Chinese with English abstract).
Sverjensky, D.A., 1986. Genesis of Mississippi Valley-type lead–zinc deposits. Annual Review of Earth and Planetary Sciences 14, 177–199.
Titley, S.R., 1993. Characteristics of high temperature carbonate-hosted massive sulfide ores in the United States, Mexico and Peru. In: Kirkham, R.V., Sinclair, W.D., Thorpe, R.I., Duke, J.M. (Eds.), Mineral Deposit Modeling. Geological Association of Canada Special Publication, pp. 585–614.
Titley, S.R., 1996. Characteristics of high temperature, carbonate-hosted replacement ores and some comparisons with Mississippi Valley-type ores. Society of Economic Geologists Special Publication 4, 244–254.
Tu, G.Z., 1984. Geochemistry of Strata-bound Ore Deposits in China (Volumes I). Science Press, Beijing, pp. 13–69 (in Chinese with English abstract).
Tu, G.Z., 1987. Geochemistry of Strata-bound Ore Deposits in China (Volumes II). Science Press, Beijing, pp. 156–160 (in Chinese with English abstract).
Tu, G.Z., 1988. Geochemistry of Strata-bound Ore Deposits in China (Volumes III). Science Press, Beijing, pp. 255–311 (in Chinese with English abstract).
Zhang, L.G., 1995. Application of Stable Isotopes in Geological Sciences. Shaanxi Science and Technology Press, Xi'an, pp. 23–245 (in Chinese with English abstract).
Zhang, W.J., 1984. A preliminary discussion on the sedimentary origin and metallogenic rule of Pb–Zn deposits in northeastern Yunnan. Journal of Geology and Exploration 7, 11–16 (in Chinese with English abstract).
Zhang, X.C., 1989. Geological characteristics and chemical composition of deep ores in the No. 1 orebody of the Kuangshanchang Pb–Zn deposit—a research report, pp. 6–54 (in Chinese).
Zhang, Y.X., Yuan, X.C., 1988. Panxi Rift. Geological Publishing House, Beijing, pp. 5–63 (in Chinese with English abstract).
Zhao, Z., 1995. Metallogenic model of Pb–Zn deposits in northeastern Yunnan. Journal of Yunnan Geology 14 (4), 350–354 (in Chinese with English abstract).
Zartman, R.E., Doe, B.R., 1981. Plumbotectonics—the model. Tectonophysics 75, 135–162.
Zhen, Q.A., 1997. Convection-circulating metallogenesis of the Kuangshanchang and Qilinchang Pb–Zn deposits at Huize and hydrothermal solution-derived massive Pb–Zn-rich orebodies—practice and understanding. Mineral Resource Geology of Southwest China 11 (1–2), 8–16 (in Chinese with English abstract).
Zhou, C.X., 1996. The origin of the mineralizing metals, the geochemical characteristics of ore-forming fluid, and the genesis of Qilinchang Zn–Pb deposit, northeast Yunnan Province, China: Unpublished M. Sc. thesis, Institute of Geochemistry, Chinese Academy of Sciences, Guiyang, 84 pp. (in Chinese with English abstract).
Zhou, C.X., Wei, C.S., Ye, Z., 1997. The Mississippi Valley-type Pb–Zn deposits. Geology–Geochemistry 17 (1), 65–75 (in Chinese with English abstract).
Zhou, C.X., Wei, S.S., Guo, J.Y., Li, C.Y., 2001. The source of metals in the Qilichang Zn–Pb deposit, northeastern Yunnan, China: Pb–Sr isotope constrains. Economic Geology 96, 583–598.